



**Thermoluminescence investigations on $x\text{Y}_2\text{O}_3 \cdot (60-x)\text{P}_2\text{O}_5 \cdot 40\text{SiO}_2$
vitroceramic compounds irradiated with electrons and mixed
neutron-gamma fields**

Ph.D. Thesis summary

Author:

Barna Biró

Supervisors:

Prof. dr. Viorica Simon

Faculty of Physics, Babeş-Bolyai University
(UBB, Cluj-Napoca, Romania)

Interdisciplinary Research Institute on Bio-Nano-
Science of the Babeş-Bolyai University
(ICI-BNS, Cluj-Napoca, Romania)

Dr. András Csaba Fenyvesi

Institute for Nuclear Research, Hungarian
Academy of Sciences
(HAS Atomki, Debrecen, Hungary)

Cluj-Napoca 2019

Table of contents

Introduction	5
Thesis statements.....	9
I. THEORY.....	11
1. Luminescence phenomena.....	11
2. Thermoluminescence of the vitroc ceramic material.....	14
2.1 The irradiation procedure.....	15
2.2 The heating procedure	16
2.3 Mathematical description of thermoluminescence phenomena.....	16
3. The nuclear physics background of neutron production at the MGC-20E cyclotron....	20
3.1 Production of neutrons.....	20
4. Determination absorbed dose by the twin ionization chamber	31
4.1 Bragg–Gray cavity theory.....	31
4.2 Determination of absorbed dose	31
5. The activation method for monitoring the neutron fluence	32
5.1 Basic formulas in neutron activation	33
II. MATERIALS AND METHODS	36
1. Production of $xY_2O_3 \cdot (60-x)P_2O_5 \cdot 40SiO_2$ vitroc ceramic compounds.....	36
2. The applied irradiation facilities	36
2.1 The electron source	36
2.2 The d+Be and the d+D fast neutron irradiation facilities	38
3. Measurement of the thermoluminescence signals.....	42
3.1 The Risø TL/OSL Luminescence Reader.....	42
3.2 Thermoluminescence measurements with the Risø TL/OSL Reader.....	43
3.3 The measurement method of the thermoluminescence signals	44
4. Methods of the characterisation of the irradiation fields.....	45

4.1	Determination of the neutron spectra.....	45
5.	<i>Applied equipment, materials and method for dosimetry measurements in the mixed n-γ fields.....</i>	46
5.1	Ionization chambers and materials, arrangement of the measurement equipment	46
5.2	Determination method of separate neutron and gamma absorbed dose with the twin ionization chamber technique in the mixed n-γ field.....	47
6.	<i>Calculation of neutron KERMA rates</i>	53
7.	<i>Monitoring the neutron fluence rate by an activation method</i>	54
7.1	The activation monitor samples.....	54
7.2	High purity coaxial germanium detector	54
7.3	Method of monitoring the neutron fluence rate by activation detectors.....	55
III.	<i>RESULTS AND DISCUSSION.....</i>	64
1.	<i>The TL investigations of the $xY_2O_3 \cdot (60-x)P_2O_5 \cdot 40SiO_2$ vitroceraamics in the β^- particles field.....</i>	65
1.1	The results obtained without pre-heating	65
1.2	The results obtained with pre-heating	72
1.3	Multiple aliquot protocol and minimum detectable dose	77
1.4	Single aliquot protocol and repeatability.....	79
1.5	Further investigation on dosimetric properties of the $30Y_2O_3 \cdot 30P_2O_5 \cdot 40SiO_2$ vitroceraamic: batch homogeneity and fading.....	82
2.	<i>Study of the $30Y_2O_3 \cdot 30P_2O_5 \cdot 40SiO_2$ vitroceraamic material in mixed n-γ fields.....</i>	84
2.1	The neutron field of the d+D irradiation facility.....	84
2.2	The neutron field of the d+Be irradiation facility	90
2.3	The irradiation experiments	92
2.4	Estimation of the neutron fluences	100
2.5	Results of the dosimetry measurements in mixed n-γ fields.....	104

3. Thermoluminescence of the $30Y_2O_3 \cdot 30P_2O_5 \cdot 40SiO_2$ vitroc ceramic material irradiated with broad spectrum $d+Be$ and quasi-monoenergetic $d+D$ neutrons.....	108
3.1 The TL glow curves obtained after the irradiations done with mixed $n-\gamma$ fields.....	108
3.2 Determination of the TL signals produced by fast neutrons and estimation of the relative neutron sensitivity of the vitroc ceramic	115
3.3 Estimation of the TL dose response of the $30Y_2O_3 \cdot 30P_2O_5 \cdot 40SiO_2$ vitroc ceramic in mixed $n-\gamma$ fields.....	121
4. Investigation of the TL of neutron irradiated $30Y_2O_3 \cdot 30P_2O_5 \cdot 40SiO_2$ vitroc ceramic with β^--particles	126
4.1 Irradiations with the $^{90}Sr-^{90}Y$ source	127
4.2 The TL glow curves of the vitroc ceramic material and the TL response as the function of the β^- absorbed doses.....	128
5. Overview of the absorbed doses delivered to the 30 mol% Y_2O_3 vitroc ceramic	141
IV. SUMMARY AND CONCLUSIONS.....	143
Acknowledgements.....	146
List of publications.....	147
List of conferences	148
References.....	149

Keywords: *thermoluminescence dosimetry, twin ionization chambers dosimetry, foil activation technique, dosimeter, $30Y_2O_3 \cdot 30P_2O_5 \cdot 40SiO_2$ vitroc ceramic material, β^- particles radiation field, mixed neutron-gamma field.*

Introduction

The presence of radioisotopes and complex nuclear radiation fields have to be considered in numerous cases e.g. in industry, radiation therapy, avionic and space activities, technologies of nuclear energetics, operation of informatics systems, research at nuclear particle accelerators, etc.. In media exposed to a radiation environment different radiation damage processes can be induced by the energetic particles of the radiation environment. The first steps of the radiation damage are excitations of the electron structures of the media and displacement of energetic atomic nuclei. Both kind of process can lead to formation of imperfections both in the electron structure and the atomic and molecular network of the media. The changes of the internal structures can lead to modification of the characteristics of the media. The knowledge of the radiation induced damages of the human body and their biological effects are especially important.

Numerous types of application specific dosimeters and dosimetry methods have been developed and available [1] [2] [3]. The increasing number of industrial, medical and agricultural applications based on the use of ultraviolet, X-rays, beta and gamma radiations account for the need to constantly search for new materials with adequate dosimetric characteristics. Radiation dosimetry with solid luminescent materials is a well-established method of monitoring ionizing radiation [4]. McKeever in the year of 1985 [5], McKeever et al. in the year of 1995 [6] and Furetta et al. in the year of 1998 [7] published a comprehensive description of the thermoluminescent properties required by a material for dosimetric purposes.

The dosimetric compounds, glass systems, polycrystalline ceramics and vitroceraics are of great interest due to their optical transparency, relatively simple preparation, easy shaping and long-term stability. Several studies were published from the investigation of the thermoluminescence properties of the borate glasses (doped with alkaline, alkaline earth, transition metal or rare-earth), the phosphate, tellurite and silicate compounds [7] [8] [9] [10] [11] [12] [13] [14] [15] [16] [17] [18] [19] [20] [21] [22] [23] [24] [25]. It was stated that luminescence materials based on silicates as host material exhibit strong chemical stability, high energy ion irradiation resistance and high UV and visible light transmittance [25]. From the viewpoint of dosimetry applications it is interesting to mention that it was observed that in the cases of borate glasses and glass-ceramics (vitroceraic) with congruent compositions that the glass-ceramics presented more defined thermoluminescent (TL) signals than the glasses [26]. This phenomenon is worth to study in the cases of other types of glasses and vitroceraics.

The scope of the present Thesis was studying the thermoluminescence (TL) of $xY_2O_3 \cdot (60-x)P_2O_5 \cdot 40SiO_2$ vitroceraamics compounds exposed to radiation fields of electrons and mixed neutron-gamma fields.

One of the motivation of my study was the nature of the vitroceraamics structure of the $xY_2O_3 \cdot (60-x)P_2O_5 \cdot 40SiO_2$ materials. In the vitroceraamic structure approximately 90% of the material is in polycrystalline phase and the crystals are embedded in the non-crystallized amorphous phase. The crystals sizes range between 0.1 and 1 μm [27] and the structure is practically void free. Taking these features into account, vitroceraamic materials present inherent advantages over the conventional glass and ceramic compounds, such as significantly small or even negative thermal expansion coefficient and improved properties under mechanical stress [28]. Adding yttrium into the composition enhances vitroceraamics characteristics because yttrium is known to play a role as an impurity gathering element due to its ability to remove excess oxygen from the bulk, and also as a trivalent component which increases the vitroceraamic system resistance to water attack [15].

Exposition of the $xY_2O_3 \cdot (60-x)P_2O_5 \cdot 40SiO_2$ materials to radiation environments with gamma photons and electrons leads to radiation induced thermoluminescence of the materials. Furthermore, Yttrium enhances the TL response of the material (the luminescence efficiency). The Yttrium is activator in the TL material and it is acts as luminescent center [29]. Therefore, studying the effect of the yttrium content on the TL response and the dose dependence of the TL response were interesting from the point of view of potential dosimetry applications of the materials. The $xY_2O_3 \cdot (60-x)P_2O_5 \cdot 40SiO_2$ vitroceraamic compounds doped with xY_2O_3 at various concentrations (0 mol%, 5 mol%, 10 mol%, 15 mol%, 20 mol% and 30 mol%) were studied. On the basis of our results the $30Y_2O_3 \cdot 30P_2O_5 \cdot 40SiO_2$ material proved to be the most suitable for TL dosimetry purposes and it was selected for further detailed studies [30].

One of the motivations of this study was the fact that $(xP_2O_5 (1-x)SiO_2)$ phosphosilicate glasses are used in many microelectronic devices (e.g. in MOSFETs) and fibre-optics systems that have to operate in harsh and complex radiation environments (e.g. spallation neutron sources [31], IFMIF-DONES / DEMO / IFMIF-EVEDA [32] [33], ITER [34]). Thus, it is important to study the radiation tolerance of these glasses. Also, it is important to search for methods that can be suitable for monitoring the radiation damage preferably using the same material with the same structure as radiation monitor [35]. For monitoring the radiation damage of these devices thermoluminescent dosimeters made of $xY_2O_3 \cdot (60-x)P_2O_5 \cdot 40SiO_2$ seem to be good choice.

In the last decade phosphosilicate glasses with high Y_2O_3 content attracted attention, too. Neutron activated microspheres of this kind of glass have been considered as new generation potential carriers of the ^{90m}Y radioisotope used for human brachytherapy applications. Christie et al. (2011) [36] and Fu and Christie [37] have demonstrated via classical molecular dynamics simulations that adding Y_2O_3 improves the stability and the durability of the glass structures.

In radiation environments with neutron component the $30Y_2O_3 \cdot 30P_2O_5 \cdot 40SiO_2$ materials can become radioactive via different nuclear reactions: $^{31}P(n,\gamma)^{32}P$, $^{31}P(n,p)^{31}Si$, $^{31}P(n,2n)^{30}P$, $^{89}Y(n,\gamma)^{90m+g}Y$, $^{89}Y(n,p)^{89}Sr$ and the $^{89}Y(n,2n)^{88}Y$. The radioactive decay of the produced radioisotopes can lead to formation of recoiled (displaced) energetic and highly ionized nuclei. These recoils can induce defects in the electronic band structure of the material, too. All these effects suggest that the $30Y_2O_3 \cdot 30P_2O_5 \cdot 40SiO_2$ material can be used both as activation and thermoluminescent neutron dosimeters. The cross sections of the neutron induced reactions depend on the neutron energy. This means that the responses of $30Y_2O_3 \cdot 30P_2O_5 \cdot 40SiO_2$ material to neutrons (induced radioactivities and thermoluminescence) have to depend not only on the neutron fluence and the absorbed neutron dose but on the neutron energy, too. Therefore, one of the aims of the present Thesis was to obtain experimental information on the neutron energy dependence of the thermoluminescence response of the $30Y_2O_3 \cdot 30P_2O_5 \cdot 40SiO_2$ material [35].

My research was performed at Faculty of Physics of Babeş-Bolyai University (Cluj-Napoca, Romania), in the Interdisciplinary Research Institute on Bio-Nano-Science of Babeş-Bolyai University and at the Hungarian Academy of Sciences Institute for Nuclear Research (HAS Atomki, Debrecen, Hungary).

This Thesis presents the background and the experimental details of my research and summarises my new results and the conclusions of my investigations in the form of 5 Thesis statements.

Thesis statements

- Detailed comparative investigations of the nuclear radiation induced thermoluminescence properties of new types of $xY_2O_3 \cdot (60-x)P_2O_5 \cdot 40SiO_2$ vitroceraamics compounds doped with Y_2O_3 at various concentrations ($x = 0, 5, 10, 15, 20, 30$ mol%) was carried out for the first time. I demonstrated that the $30Y_2O_3 \cdot 30P_2O_5 \cdot 40SiO_2$ vitroceraamic material gives the highest thermoluminescent response to unit absorbed dose of β^- -particles and, of the six investigated materials, this

material is the most suitable for dosimetry purposes. This vitroceraamics exhibited the less complicated glow curve structure. The dominant high-temperature peak presents the brightest signals and the best degree of linearity (from 0.75 Gy to 9 Gy). This vitroceraamics material has acceptable batch homogeneity, poor fading of the signal, good repeatability and the minimum detectable absorbed dose is a few mGy [30].

- I have developed an experimental method for investigating the characteristics of the thermoluminescence response of the $30\text{Y}_2\text{O}_3\cdot 30\text{P}_2\text{O}_5\cdot 40\text{SiO}_2$ vitroceraamic material exposed to mixed n- γ fields. The studies were carried out using broad spectrum d+Be neutrons and quasi-monoenergetic d+D neutrons. I used a neutron activation method for monitoring the neutron fluences and a twin ionization chamber technique for measuring the separate neutron and gamma absorbed-dose rates [35].
- I validated the relevant neutron spectra of the d+Be and d+D neutron sources that were obtained either from extrapolation of the data of Brede et al. [38] (d+Be) or interpolation of the data taken from Reimer [39] (d+D). The saturation activities were calculated (C) using the neutron spectra of the d+Be and d+D neutron sources and the excitation functions of the monitor nuclear reactions. The measured saturation activities (E) were compared with the calculated (C) ones. The results of the comparisons (C/E) validated the neutron spectra obtained in the present study [35].
- Estimations for the relative neutron sensitivity of the $30\text{Y}_2\text{O}_3\cdot 30\text{P}_2\text{O}_5\cdot 40\text{SiO}_2$ vitroceraamic material in the cases of the broad spectrum d+Be ($E_n = 0\text{--}14.5$ MeV) and the quasi-monoenergetic ($E_n = 12.4 \pm 0.22$ MeV) d+D neutron sources were carried out. The obtained results suggest that the relative neutron sensitivity depends on the neutron energy [35]. Furthermore, in the cases of the two neutron sources the obtained results suggest that the estimated TL dose responses of the vitroceraamic as a function of the neutron, gamma and total absorbed doses are linear within uncertainties of the dosimetry measurements.
- I studied the possible effect of the fast neutron induced displacement damage on the TL response of the 30 mol% Y_2O_3 vitroceraamic to β^- particles. In the first step samples

never irradiated before were exposed to β^- -particles and the absorbed doses were in the $D_\beta = 0.75 - 1000$ Gy range. In the second step samples irradiated before with $D_n = 80 - 110$ Gy neutron absorbed dose range were selected and exposed to β^- -particles and the absorbed doses were in the $D_\beta = 0.75 - 500$ Gy range. The results obtained in the two cases were compared. It was found that the TL properties of the non-irradiated and neutron irradiated samples of the 30 mol% Y_2O_3 vitroceraamics agreed within the uncertainty of the measurements. In other words, no statistically significant effect of the neutron induced damage on the TL properties of the material was observed.

I. RESULTS AND DISCUSSION

The thesis summary reports the results that were achieved studying the TL properties of the $xY_2O_3 \cdot (60-x)P_2O_5 \cdot 40SiO_2$ ($0 \leq x \leq 30$ mol%) vitroceraamics compounds in β^- and mixed n- γ radiation fields. The following results are presented:

Beta electron field

- the TL glow curves and the dose response in the 0.75 Gy - 9 Gy absorbed doses region measured at $x = 0\%$, 5%, 10%, 15%, 20%, 30% Y_2O_3 concentrations via the single aliquot protocol (without preheat and with preheat),
- the dose responses measured with the 20 mol% Y_2O_3 and 30 mol% Y_2O_3 vitroceraamics in the 0.75 Gy - 9 Gy absorbed doses region via the single aliquot protocol and the multiple aliquot protocol,
- the repeatability test of the 20 mol% Y_2O_3 and 30 mol% Y_2O_3 vitroceraamics and the measurements performed via the single aliquot protocol,
- the TL glow curves and dose responses measured with the 30 mol% Y_2O_3 vitroceraamics in the 0.75 Gy - 9 Gy (low dose) and the 15 Gy - 1000 Gy (high dose) absorbed dose ranges, after the experiments in the mixed n- γ fields.

Mixed neutron-gamma fields

- validation the neutron spectra of the d+Be and the d+D neutron sources,
- results of dosimetry measurements in mixed n- γ fields,
- the TL glow curves measured with the vitroceraamics with $x = 30$ mol% Y_2O_3 ,
- determination the TL signals induced by fast neutrons in the vitroceraamics with $x = 30$ mol% Y_2O_3 material,

- determination of the relative neutron sensitivity of the vitroceramics with $x = 30$ mol% Y_2O_3 for irradiations with two different neutron sources,
- determination of the relative neutron sensitivity as a function of the neutron energy in the case of the vitroceramics with $x = 30$ mol% Y_2O_3 ,
- estimated the TL dose response of the vitroceramics with $x = 30$ mol% Y_2O_3 as a function of the neutron, gamma and total absorbed dose.

1. The TL investigations of the $xY_2O_3 \cdot (60-x)P_2O_5 \cdot 40SiO_2$ vitroceramics in the β^- particles field

Thermoluminescence glow curves

TL glow curves were recorded at a controlled heating rate (5 °C/s) after beta irradiation to 6 Gy both with and without applying thermal treatments. During reading out of the TL signal, the sample was heated to 500 °C. Upon irradiation, bright TL signals have been displayed by most samples, with multiple TL emissions both in the low (100 °C) temperature range as well as in the dosimetric interval (200 °C and above). The shape of the glow curve is changed by adding Y_2O_3 , with an increased relative importance of the high temperature peaks although there is no clear trend with concentration. As the low temperature TL peaks are not expected to be thermally stable and decay in a period of tens of hours, a time similar to the storage time of regular dosimeters before readout, we have applied a thermal treatment in order to remove these unstable signals and to recreate the possible charge transfer from the low temperature traps to the high temperature peaks during storage. The thermal treatment consisted of a preheat with a duration of 10 s at 150 °C for samples doped with 0–15 mol% Y_2O_3 and to 175 °C in the case of 20 mol% Y_2O_3 and 30 mol% Y_2O_3 , respectively. **Figure 1-1** presents a comparison among the samples glow curves as function of Y_2O_3 concentration (0–30 mol%) following the thermal treatment and without the thermal treatment. It can be noted that the glow curve structure is less complicated in the case of 20 mol% Y_2O_3 and 30 mol% Y_2O_3 and the increased concentration leads to brighter signals. The glow curve recorded for the $30Y_2O_3 \cdot 30P_2O_5 \cdot 40SiO_2$ compound was similar in terms of structural simplicity (showing one dominant high-temperature peak) and position of the dosimetric peak (placed around 220 °C) with the glow curve obtained from the MCP-7 standard thermoluminescent dosimeter.

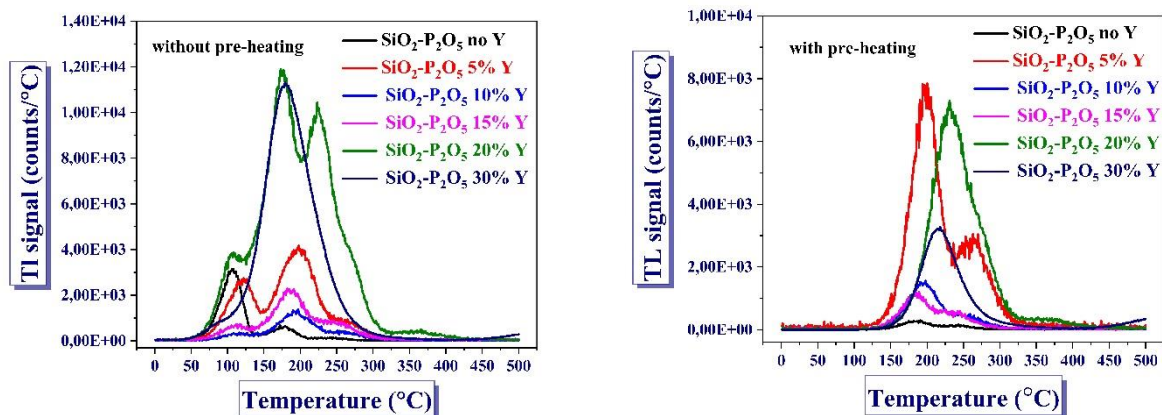


Figure 1-1. Comparison of the TL glow curves obtained with the vitroceraamics samples that have different Y_2O_3 concentration. The glow curve for 30 mol% Y_2O_3 was normalized to 1 mg while the other TL glow curves were normalized to 10 mg sample mass.

Multiple aliquot protocol and minimum detectable dose

Based on glow curves structure and brightness, the dose dependence of the $20Y_2O_3 \cdot 40P_2O_5 \cdot 40SiO_2$ and $30Y_2O_3 \cdot 30P_2O_5 \cdot 40SiO_2$ TL signals was further studied in a multiple aliquot procedure, the rest of the concentrations being discarded due to their poorer dosimetric characteristics. A set of aliquots was prepared and for each applied dose (0.75, 1.5, 3, 6, 9 Gy) a different number of fresh aliquots was used ($n = 1-15$). Samples have been individually irradiated with the built-in $^{90}Sr-^{90}Y$ beta source and the TL signals have been recorded. The selected region of interest was 150–300 °C. As shown in **Figure 1-2**, both samples exhibited a linear dose response relationship in the investigated dose range (0.75–9 Gy). The sensitivities obtained for 10 mg of material were $S = 79596$ counts/Gy for $20Y_2O_3 \cdot 40P_2O_5 \cdot 40SiO_2$ and $S = 760478$ counts/Gy for $30Y_2O_3 \cdot 30P_2O_5 \cdot 40SiO_2$, respectively.

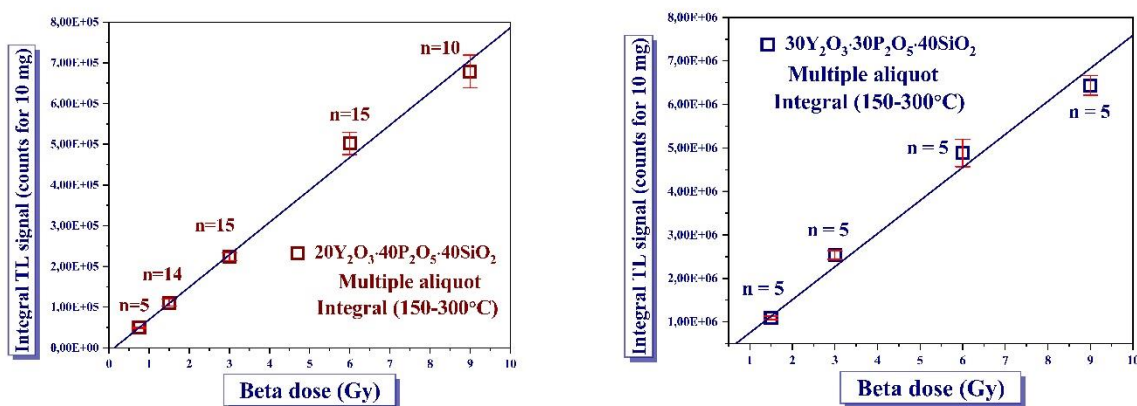


Figure 1-2. The dose response of the 20 mol% Y_2O_3 and the 30 mol% Y_2O_3 vitroceraamics, as a function of the delivered absorbed doses (0.75, 1.5, 3, 6 and 9 Gy). The n denotes the number of aliquots applied for each absorbed dose.

The minimum detectable dose (MDD) was calculated as the dose for which the signal is three times the standard deviation of the corresponding background. In the case of $20\text{Y}_2\text{O}_3\cdot 40\text{P}_2\text{O}_5\cdot 40\text{SiO}_2$ the estimated MDD for instantaneous measurements was 16 mGy, while for the $30\text{Y}_2\text{O}_3\cdot 30\text{P}_2\text{O}_5\cdot 40\text{SiO}_2$ a value of 4 mGy was obtained.

Single aliquot protocol and repeatability

Using a thermoluminescence dosimeter in a single aliquot protocol requires much more sample material, is less time consuming and gives a better precision. In a single aliquot protocol the accrued dose and the dose response can be constructed on one single portion of material as long as the samples are characterised by a satisfactory repeatability. In order to apply such a protocol on the investigated samples, the presence of a sensitization or desensitization trend for 20 mol% Y_2O_3 and 30 mol% Y_2O_3 vitroceraamics, respectively was further tested. In the cases of using these vitroceraamic materials repeated irradiation-readout cycles were performed irradiating the aliquots with 6 Gy absorbed dose and there was no waiting time between the irradiation and the readout. The integrated TL_n signal obtained in the case of the n-th measurement cycle and normalized for 10 mg was compared with the integrated TL_1 value obtained from the initial (1st) measurement cycle and normalized to 10 mg. One can conclude that sensitization was observed in the case of the $20\text{Y}_2\text{O}_3\cdot 40\text{P}_2\text{O}_5\cdot 40\text{SiO}_2$ vitroceraamic and the sensitization increased up to 46% after ten measurement cycles. In the case of the $30\text{Y}_2\text{O}_3\cdot 30\text{P}_2\text{O}_5\cdot 40\text{SiO}_2$ vitroceraamic desensitization was observed and the desensitization decreased to 9% after ten measurement cycles (good repeatability). The results presented in

Figure 1-3.

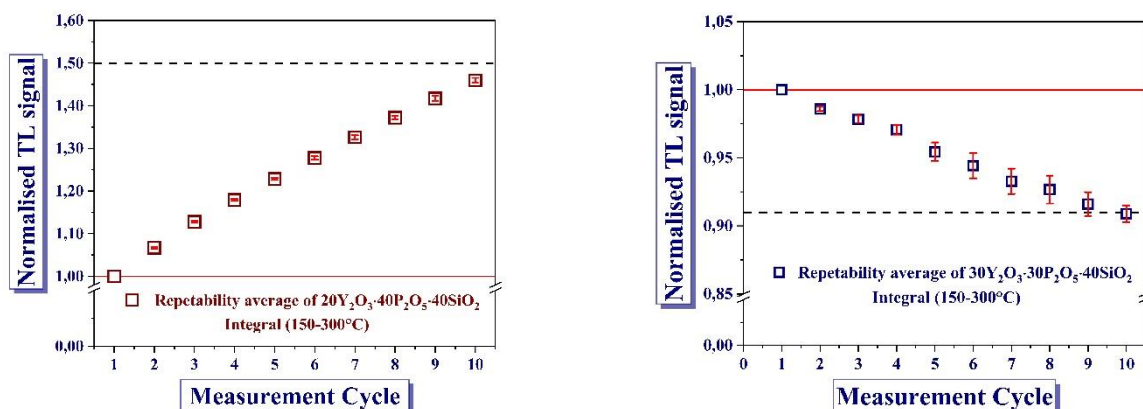


Figure 1-3. Results of the repeatability test in the case of $20\text{Y}_2\text{O}_3\cdot 40\text{P}_2\text{O}_5\cdot 40\text{SiO}_2$ (a) – average response of 6 aliquots and $30\text{Y}_2\text{O}_3\cdot 30\text{P}_2\text{O}_5\cdot 40\text{SiO}_2$ (b) – average response of 5 aliquots.

The TL dose response of both vitroceraamic material (20 mol% Y_2O_3 and 30 mol% Y_2O_3) was studied by a single aliquot regeneration protocol. The TL signal was integrated for the 150

– 300 °C temperature region. The absorbed doses were 0.75, 1.5, 3, 6 and 9 Gy. In the case of $20\text{Y}_2\text{O}_3\cdot 40\text{P}_2\text{O}_5\cdot 40\text{SiO}_2$ five different aliquots were used. Eight aliquots were used in the case of the $30\text{Y}_2\text{O}_3\cdot 30\text{P}_2\text{O}_5\cdot 40\text{SiO}_2$ material. The TL response was linear function of the absorbed dose for both material. The dose responses are shown in **Figure 1-4**, where each data point represents averaged TL signal.

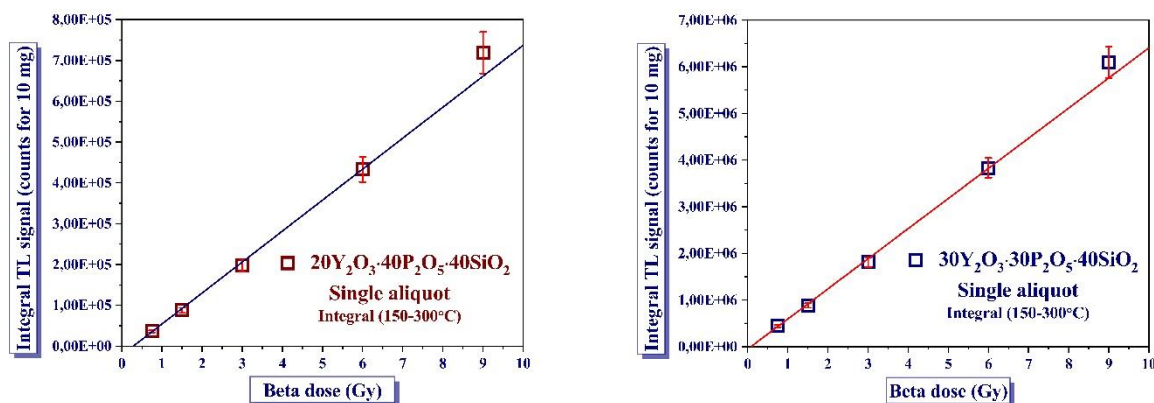


Figure 1-4. The TL responses obtained by the single aliquot regenerative dose protocol and applying preheat (for 10 s at 175 °C).

In the case of the single regeneration aliquot protocol, the average sensitivity of $30\text{Y}_2\text{O}_3\cdot 30\text{P}_2\text{O}_5\cdot 40\text{SiO}_2$ vitrocereamics was ~ 650,000 cts for 10 mg/Gy. This value is consistent within 2σ with the average sensitivity obtained with the multiple aliquot procedure (~ 760,000 cts for 10 mg/Gy). Furthermore, the average sensitivity of the $20\text{Y}_2\text{O}_3\cdot 40\text{P}_2\text{O}_5\cdot 40\text{SiO}_2$ vitrocereamics was ~ 76,000 cts for 10 mg/Gy. This value is consistent within 2σ with the average sensitivity that was obtained with the multiple aliquot procedure (~ 80,000 cts for 10 mg/Gy). From these results it can be seen, that the dosimetric properties of 30 mol% and 20 mol% Y_2O_3 vitrocereamic can be determined by the single aliquot regenerative protocol.

It can be concluded that the 20 mol% Y_2O_3 vitrocereamic shows a lower TL glow curve and the sensitivity of the material is lower by one order of magnitude than that of the $30\text{Y}_2\text{O}_3\cdot 30\text{P}_2\text{O}_5\cdot 40\text{SiO}_2$ material. The sensitivity of the 20 mol% Y_2O_3 vitrocereamic increased significantly (up to 46% after ten cycles) during the repeatability test. Therefore, our further investigations focused exclusively on the $30\text{Y}_2\text{O}_3\cdot 30\text{P}_2\text{O}_5\cdot 40\text{SiO}_2$ vitrocereamic material.

Further investigation on dosimetric properties of the $30Y_2O_3 \cdot 30P_2O_5 \cdot 40SiO_2$ vitroc ceramic: batch homogeneity and fading

The batch homogeneity and the fading study for the $30Y_2O_3 \cdot 30P_2O_5 \cdot 40SiO_2$ vitroc ceramic were performed using fresh material. About 1 g of material was irradiated with approximately

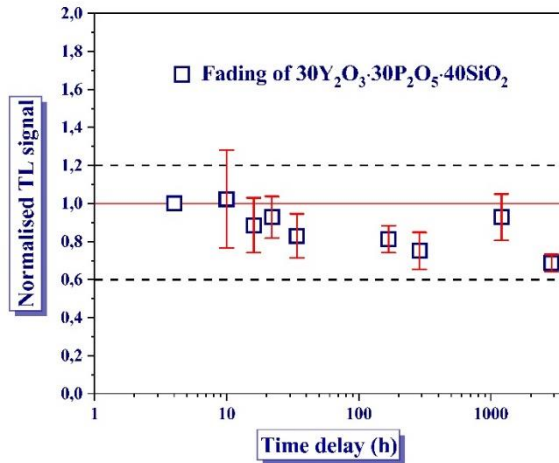


Figure 1-5. The fading of the $30Y_2O_3 \cdot 30P_2O_5 \cdot 40SiO_2$ vitroc ceramic. The uncertainty bars correspond to three times of the standard uncertainty of the mean value (3σ).

3 Gy absorbed dose in a homogeneous field of ^{60}Co gamma photons. After irradiation the TL measurements were carried out instantaneously and then 10 h, 16 h, 22 h, 34 h, 168 h, 288 h, 1200 h and 2880 h after the end of the irradiation. Before reading out the samples they were stored in dark at room temperature. Different numbers of aliquots (5 – 15) were used for the different measurements. After four months the fading reached $\sim 70\%$. The relative standard deviation of the

integrated and normalized TL signals varied between 10% and 28%. The fading results are presented in **Figure 1-5**.

2. Study of the $30Y_2O_3 \cdot 30P_2O_5 \cdot 40SiO_2$ vitroc ceramic material in mixed n- γ fields

The TL response of the $30Y_2O_3 \cdot 30P_2O_5 \cdot 40SiO_2$ vitroc ceramic material was studied in mixed n- γ fields of the d+D and d+Be fast neutron irradiation facilities at the MGC-20E cyclotron, too. Broad spectrum d+Be ($E_n = 0 - 14.5$ MeV) and quasi-monoenergetic d+D ($E_n = 12.4 \pm 0.22$ MeV) neutrons were used. Six irradiation experiments were carried out. The 1st, 3rd and 5th irradiations were done at the d+Be neutron source. The d+D neutron source was used in the 2nd, 4th and 6th irradiations.

The irradiation experiments

The powder samples of the vitroc ceramics were placed in 0.1 mm thick polyethylene sachets. Then they were fixed on a 1 mm thick support plate made of AlMgSi alloy. The thicknesses of the specimens were about 1 mm. For monitoring the neutron fluences high purity aluminium (Al) and iron (Fe) discs were fixed behind the TL sample on the back side of the

support plate. **Figure 2-1** shows the general sketches of the arrangements of the irradiations and the dosimetry checks at the different neutron sources used.

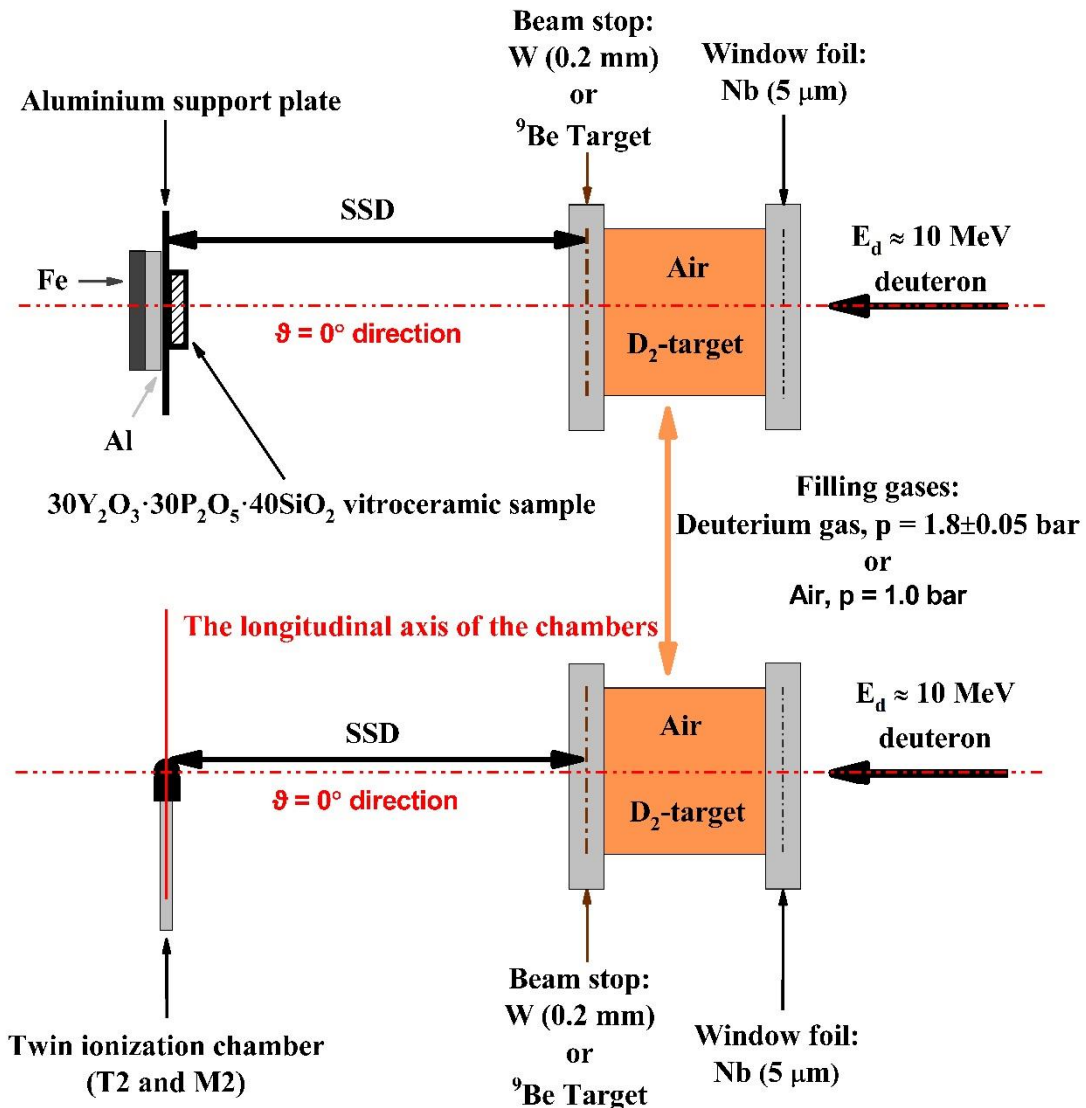


Figure 2-1. The general sketches of the arrangements of the irradiations (upper) and the dosimetry checks (below) performed at the quasi-monoenergetic d+d neutron source and at the broad spectrum d+Be neutron source.

The geometry center of the support plate was positioned to the $\vartheta = 0^\circ$ direction (the direction of the bombarding beam) and the support plate was perpendicular to the $\vartheta = 0^\circ$ direction. The source-to-sample distance (SSD) was the distance measured from the geometry center of the target along the $\vartheta = 0^\circ$ direction.

A pair of twin ionization chambers (twin ionization chambers) were employed for determining the separate neutron (D_N) and gamma (D_G) absorbed dose at the irradiation positions (SSD) of the 30 mol% Y_2O_3 vitroc ceramic samples. The dosimetry measurements were performed before and after irradiation of the TL samples. The measurements were carried out

separately with the T2 and M2 ionization chambers. The geometry centers of the chambers were positioned to the $\vartheta = 0^\circ$ horizontal direction and the longitudinal axes of the chamber was perpendicular to the $\vartheta = 0^\circ$ direction. The sample-to-source distance (SSD) of the chambers was the same than that of the vitroceramic samples.

Estimation of the neutron fluences

Al and Fe discs were irradiated with the vitroceramic samples for monitoring the neutron fluences. The Al and Fe discs were activated via the $^{56}\text{Fe}(n,p)^{56}\text{Mn}$, $^{27}\text{Al}(n,p)^{27}\text{Mg}$ and $^{27}\text{Al}(n,\alpha)^{24}\text{Na}$ nuclear reactions. The nuclear data and their uncertainties were taken from the WWW Table of Radioactive Isotopes evaluated by Chu et al. (1999) [40]. After irradiation the gamma activities of the discs were measured with a calibrated HPGe detector. The full energy photopeaks were counted. Then the saturation activities of the ^{56}Mn , ^{27}Mg and ^{24}Na radioisotopes were determined. The obtained results were used for estimating the neutron fluence delivered to the vitroceramic sample. Also, the saturation activities were calculated using the neutron spectra of the d+Be and d+D neutron sources [35] and the excitation functions of the monitor nuclear reactions. The measured saturation activities were compared with the calculated saturation activities. This method was used for validation of the estimated neutron spectra, too.

Figure 2-2 shows the extrapolated neutron spectrum [35] and the data taken from Brede et al [38] for extrapolation of spectrum in the case of d+Be neutrons. Furthermore, **Figure 2-2** shows interpolated neutron spectrum [35] and the data taken from the published PhD thesis by Peter Reimer [39] for interpolation of spectrum in the case of d+D neutrons. The D₂-gas target used by Reimer was identical with the target used in our studies.

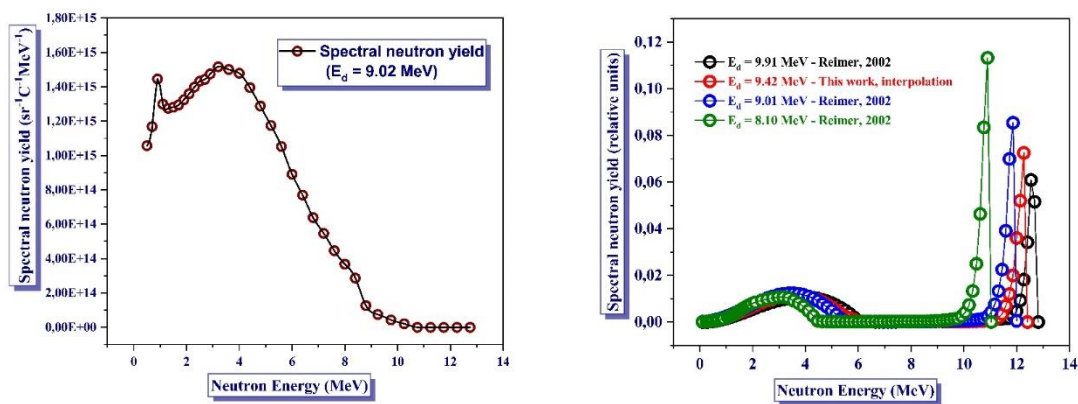


Figure 2-2. Spectral neutron yields of the d+Be and the d+D neutrons at the $\vartheta = 0^\circ$ direction.

The extrapolated spectrum of the d+Be neutrons and the interpolated spectrum of the d+D neutrons spectra were used for calculation of the expected neutron fluence rates, saturation activities and neutron KERMA rates.

The measured and calculated saturation activities

The excitation function data for the monitor nuclear reactions were taken from the ENDF/B-VII.1 library [41]. The FGM gamma spectrum evaluation code (Székely, 1985) [42] was used for determining the net area of the full energy photopeaks.

Table 2-1 lists the calculated (C) saturation activities, the averaged experimental (E) saturation activities, the (C/E) ratios and the estimated uncertainties obtained from the activity measurements, as well as the neutron fluence rates resulted from the spectrum adjustment procedures. The received neutron fluence rates refer to the centre of the vitroceraamic sample. The C/E ratios show that the agreement between the calculated and measured saturation activities was within the uncertainty of the activity measurements in the cases of Irradiation 1 and 2. Furthermore, the C/E ratios can be considered as a kind of validation of the expected neutron spectra, too. In the case of the validation of the broad spectrum of the d+Be neutron source, the difference between the calculated and averaged experimental saturation activities was $\pm 3\%$ or less (Irradiation 1). In the case of the validation of the neutron spectrum of the quasi-monoenergetic d+D neutron source the agreements between calculated and averaged experimental saturation activities were within $\pm 5\%$ (Irradiation 2).

Table 2-1. The calculated (C) and averaged experimental (E) saturation activities and the C/E ratios. E_d is the deuteron energy.

Neutron source	Number of irradiation	E_d (MeV)	Target	Nuclear reaction	Saturation activity (Bq)			Neutron fluence rate ($\text{cm}^{-2}\text{s}^{-1}$)
					Calculated	Experiment	C/E	
d+Be	1	9.02	Be d = 3 mm	$^{27}\text{Al}(\text{n,p})^{27}\text{Mg}$	3.55E+03	3.49E+03 \pm 8%	1.02	1.2E+07 \pm 8%
				$^{27}\text{Al}(\text{n},\alpha)^{24}\text{Na}$	8.45E+02	8.70E+02 \pm 6%	0.97	
				$^{56}\text{Fe}(\text{n,p})^{56}\text{Mn}$	8.74E+02	8.49E+02 \pm 8%	1.03	
	3	8.64		$^{27}\text{Al}(\text{n,p})^{27}\text{Mg}$	Not calc.	1.84E+04 \pm 4%	N/A	Not calculated [†]
				$^{27}\text{Al}(\text{n},\alpha)^{24}\text{Na}$	Not calc.	5.34E+03 \pm 8%	N/A	
				$^{56}\text{Fe}(\text{n,p})^{56}\text{Mn}$	Not calc.	1.11E+04 \pm 4%	N/A	
	5	9.04		$^{27}\text{Al}(\text{n,p})^{27}\text{Mg}$	3.70E+04	3.54E+04 \pm 2%	1.04	1.2E+08 \pm 10%
				$^{27}\text{Al}(\text{n},\alpha)^{24}\text{Na}$	8.80E+03	9.91E+03 \pm 2%	0.89	
				$^{56}\text{Fe}(\text{n,p})^{56}\text{Mn}$	9.10E+03	9.67E+03 \pm 4%	0.94	
d+D	2	9.42	D ₂ -gas p = 1.8 \pm 0.05 bar	$^{27}\text{Al}(\text{n,p})^{27}\text{Mg}$	1.03E+04	1.04E+04 \pm 7%	0.99	4.2E+06 \pm 10%
				$^{27}\text{Al}(\text{n},\alpha)^{24}\text{Na}$	1.28E+04	1.22E+04 \pm 10%	1.05	
				$^{56}\text{Fe}(\text{n,p})^{56}\text{Mn}$	7.74E+03	8.10E+03 \pm 6%	0.96	
	4	9.35		$^{27}\text{Al}(\text{n},\alpha)^{24}\text{Na}$	4.59E+03	5.48E+03 \pm 5%	0.84	4.3E+06 \pm 10%
				$^{56}\text{Fe}(\text{n,p})^{56}\text{Mn}$	2.82E+03	3.11E+03 \pm 3%	0.91	
	6	9.37		$^{27}\text{Al}(\text{n},\alpha)^{24}\text{Na}$	7.72E+03	6.96E+03 \pm 6%	1.10	6.7E+06 \pm 10%
				$^{56}\text{Fe}(\text{n,p})^{56}\text{Mn}$	4.74E+03	4.23E+03 \pm 4%	1.12	

[†]No extrapolated spectrum was available.

Results of the dosimetry measurements in mixed n-γ fields

Estimation of the relative neutron sensitivity of the TL signals of the vitroceraamics irradiated in mixed neutron-gamma fields of the d+Be and d+D neutron sources needs the determination of the separate neutron and gamma absorbed doses. The neutron absorbed dose can be calculated from the neutron spectrum and from dosimetry measurements.

The twin ionization chamber technique described by Broerse et al. (1981) [43] and Wootton et al. (1980) [44] was used for determining the separate neutron and gamma absorbed dose for the positions where the vitroceraamic were irradiated. Thimble type ionization chambers (EXRADIN T2 and M2) were employed. The two chambers have identical geometry with 0.55 cm³ sensitive volume (cavity). The material of the T2 chamber (TE-TE chamber) was made of Shonka A-150 electrically conducting plastic (Shonka et al., 1958) [45], which is approximately human striated muscle tissue equivalent (TE) material [43]. The filling gas mixture was the tissue equivalent gas mixture [43]. The material of the M2 chamber (Mg-Ar chamber) was made of magnesium. The filling gas was the argon gas.

Table 2-1. Results of the dosimetry measurements and dosimetry calculations.

n-γ fields	Number of irradiation	SSD (mm)	Twin ionization chambers (EXRADIN T2 and M2)			From evaluated data
			Measured absorbed doses			Calculated
			D _N (Gy)	D _G (Gy)	D _{N+G} (Gy)	K* (Gy)
d+Be	1	259	2.51 ± 8%	0.24 ± 14%	2.75 ± 16%	2.81**
	3	259	8.12 ± 8%	1.34 ± 14%	9.46 ± 16%	Not calc.†
	5	259	84.19 ± 8%	13.91 ± 14%	98.10 ± 16%	108.6**
d+D	2	93.3	1.49 ± 8%	0.18 ± 14%	1.67 ± 16%	1.43***
	4	88.3	4.50 ± 8%	0.63 ± 14%	5.13 ± 16%	4.99***
	6	91.3	25.55 ± 8%	5.27 ± 14%	30.82 ± 16%	23.17***

* Calculated for Shonka A-150 plastic applying the KERMA factors published by Chadwick et al. [46].

** Estimated applying the extrapolated spectrum for E_d = 9.02 MeV. The spectrum was extrapolated from the measured data published by Brede et al. [38].

*** Estimated applying the interpolated spectrum for E_d = 9.42 MeV. The spectrum was interpolated from the calculated data published by Reimer [39]. The contribution of break up neutrons produced in the W beam stop of the D2-gas target was not included.

† No extrapolated spectrum was available.

The energy distributions of the fluence rates of the d+D and d+Be neutrons and the fluence to KERMA conversion factors were used for neutron KERMA estimation. The

elemental fluence to KERMA conversion factors were taken from the literature (Chadwick et al. [46]). The obtained neutron KERMA rates refer to the positions where the vitroceraamics sample was irradiated.

The obtained measured neutron absorbed doses were compared with neutron KERMA values. The neutron absorbed doses and the neutron KERMA values refer to the Shonka A-150 plastic. For each irradiation of the $30\text{Y}_2\text{O}_3 \cdot 30\text{P}_2\text{O}_5 \cdot 40\text{SiO}_2$ vitroceraamic material the measured neutron and gamma absorbed doses and the estimated KERMA values are shown in **Table 2-1**.

3. Thermoluminescence of the $30\text{Y}_2\text{O}_3 \cdot 30\text{P}_2\text{O}_5 \cdot 40\text{SiO}_2$ vitroceraamic material irradiated with broad spectrum d+Be and quasi-monoenergetic d+D neutrons

On the basis of the obtained results the relative neutron sensitivities of the 30 mol% Y_2O_3 vitroceraamic were estimated both for the d+D and d+Be neutrons used in our studies. The results suggest that the relative neutron sensitivity of the TL material depends on the neutron energy.

After each irradiation different number of aliquots were prepared for measurements of the TL signals. Before reading out of the irradiated samples a thermal treatment was applied, that was a preheat at 175 °C for 10 s. Then the sample was heated up to 500 °C at 5 °C/s (heating rate). The TL signals were integrated in the 150 °C to 300 °C temperature range. Both TL glow curves and the integrated TL signals were normalized to 10 mg sample mass.

The TL glow curves obtained after the irradiations done with mixed n- γ fields

The shapes of the measured TL glow curves were compared with the TL glow curves obtained from the experiments done with beta electrons. It can be concluded that in the 150 °C to 300 °C temperature region:

- the shape of the averaged normalized TL glow curves of the aliquots is practically independent of
 - the neutron spectrum,
 - the absorbed neutron dose.
- the shape of the averaged normalized TL glow curves of the aliquots is very similar to the averaged normalized TL glow curves obtained from the measurements done with beta electrons.

Thus, the 150 °C to 300 °C temperature region is suitable for obtaining the integrated TL signal both in the case of the beta electrons and the mixed n- γ fields of the d+D and d+Be neutrons. It has to be mentioned that the TL glow curves measured after Irradiation 6 were slightly different

from the TL glow curves measured after Irradiation 5. The difference can be observed above 300 °C. The reason for the difference has not been understood. **Figure 3-1** shows the averaged and normalized TL curves with their standard deviations.

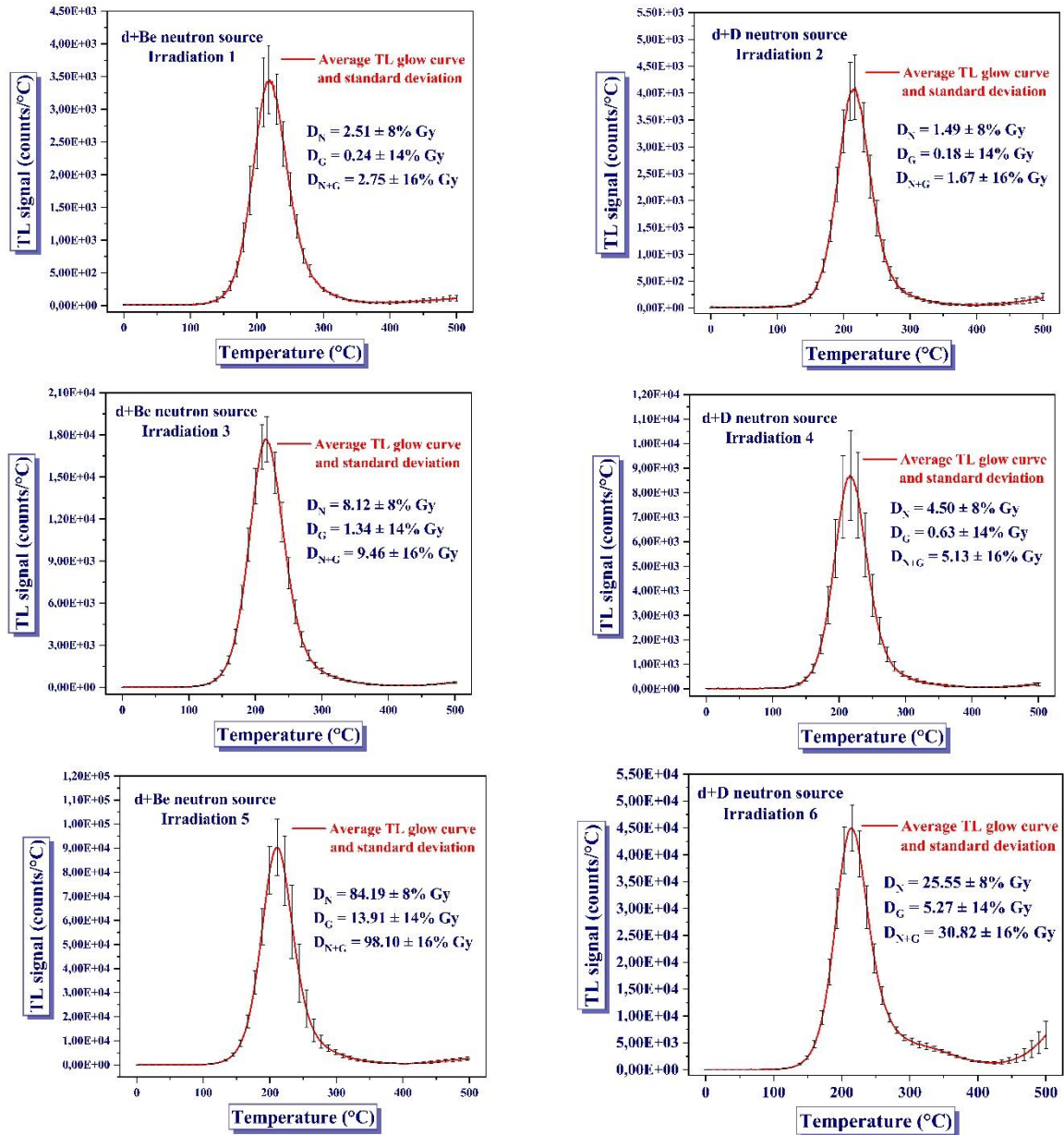


Figure 3-1. The averaged and normalized TL curves obtained after irradiations. The irradiation was done in the mixed n- γ fields of the broad spectrum the d+Be neutron source and quasi-monoenergetic d+D neutron source. The standard deviations were plotted for 10 °C broad intervals.

Determination of the TL signals produced by fast neutrons and estimation of the relative neutron sensitivity of the vitroc ceramic

In the case of the mixed n- γ fields both the gamma photons and the neutrons could contribute to the obtained TL signal. The net mass normalized \overline{TL}_{N+G} signal induced by the mixed n- γ irradiation field was calculated as the difference of the mass normalized $\overline{TL}_{N+G;norm}^{sample}$ signal obtained for the sample and the mass normalized $\overline{TL}_{norm}^{reference}$ signal obtained for the unirradiated control sample:

$$\overline{TL}_{N+G} = \overline{TL}_{N+G;norm}^{sample} - \overline{TL}_{norm}^{reference} \quad \text{Eq. 3-1}$$

The calculation of the contribution of the TL signal attributed to the gamma absorbed dose was based on the gamma absorbed dose measurements performed by twin ionization chambers and the measured S beta/gamma TL sensitivity of the material (i.e. S = 760478 cts/Gy for 10 mg) as

$$TL_G = S * D_G \quad \text{Eq. 3-2}$$

The TL_N contribution of the neutron component of the mixed n- γ field was estimated using the calculated TL_G value and the measured \overline{TL}_{N+G} . Then the TL_N value was calculated as

$$TL_N = \overline{TL}_{N+G} - TL_G \quad \text{Eq. 3-3}$$

The k_V relative neutron sensitivity of the 30 mol% Y_2O_3 vitroc ceramic was estimated as

$$k_V = \frac{R_{N/G}}{R_D} = \frac{(TL_N/TL_G)}{(D_N/D_G)} \quad \text{Eq. 3-4}$$

Table 3-1 summarizes the results of the dosimetry measurements and the TL measurements with the 30 mol% Y_2O_3 vitroc ceramics irradiated in the mixed n- γ fields. In the cases of the irradiation of the 30 mol% Y_2O_3 vitroc ceramic samples at the d+Be neutron source the obtained relative neutron sensitivities were in the $(k_V)_{d+Be} = 0.030 - 0.035$ range. Their uncertainties were in the 26% – 30% range. The averaged relative neutron sensitivity of vitroc ceramic sample was $(\bar{k}_V)_{d+Be} = 0.032 \pm 7\%$ where the indicated 7% is the relative standard deviation of the $(k_V)_{d+Be}$ values. In the cases of the irradiation of the 30 Y_2O_3 mol% vitroc ceramic samples at the d+D neutron source the obtained relative neutron sensitivities were in the $(k_V)_{d+D} = 0.127 - 0.156$ range. Their uncertainties were in the 27% – 30% range. The averaged relative neutron sensitivity of vitroc ceramic sample was $(\bar{k}_V)_{d+D} = 0.136 \pm 10\%$ where the indicated 10% is the relative standard deviation of the $(k_V)_{d+D}$ values.

Table 3-1. Results of the irradiation experiments performed in mixed n- γ field with the $30Y_2O_3 \cdot 30P_2O_5 \cdot 40SiO_2$ vitroceraic. *Irr. ID* is the ID number of the irradiation. The \bar{k}_V is the averaged relative neutron sensitivity of vitroceraic material.

n- γ field	Irr. ID	Sample ID	Twin ionization chambers (EXRADIN T2 and M2)		Thermoluminescent vitroceraics ($30Y_2O_3 \cdot 30P_2O_5 \cdot 40SiO_2$)				
			Absorbed dose		Relative neutron sensitivity				
			Measured		Calculated				
			D_N (Gy)	D_G (Gy)	net \bar{TL}_{N+G} (counts/10 mg)	TL _G (counts/10 mg)	TL _N (counts/10 mg)	k_V	\bar{k}_V
d+Be	1	1	$2.51 \pm 8\%$	$0.24 \pm 14\%$	$227892 \pm 15\%$	$171378 \pm 14\%$	$56514 \pm 21\%$	$0.032 \pm 30\%$	$0.032 \pm 7\%$
	3	1	$8.12 \pm 8\%$	$1.34 \pm 14\%$	$1194725 \pm 10\%$	$1008556 \pm 14\%$	$186168 \pm 17\%$	$0.030 \pm 27\%$	
		3 [†]			$1348295 \pm 7\%$		$339739 \pm 16\%$	$0.056^\dagger \pm 26\%$	
	5	1	$84.19 \pm 8\%$	$13.91 \pm 14\%$	$5573635 \pm 16\%$	$4600930 \pm 14\%$	$972705 \pm 21\%$	$0.035 \pm 30\%$	
		3			$5426488 \pm 8.5\%$		$825558 \pm 16\%$	$0.030 \pm 27\%$	
	d+D	2	1	$1.49 \pm 8\%$	$0.18 \pm 14\%$	$262458 \pm 14\%$	$125750 \pm 14\%$	$136708 \pm 20\%$	
4		1 [†]	$4.50 \pm 8\%$	$0.63 \pm 14\%$	$535761 \pm 14\%$	$467965 \pm 14\%$	$67796 \pm 20\%$	$0.020^\dagger \pm 29\%$	
		3			$891422 \pm 12\%$		$423457 \pm 18\%$	$0.127 \pm 28\%$	
6		1	$25.55 \pm 8\%$	$5.27 \pm 14\%$	$2772283 \pm 16\%$	$1702163 \pm 14\%$	$1070121 \pm 21\%$	$0.130 \pm 30\%$	
		3			$2990635 \pm 10\%$		$1288473 \pm 17\%$	$0.156 \pm 27\%$	

[†]Outlier data that has not been understood. The data was not used for calculation of the averaged relative neutron sensitivity.

Despite of the large uncertainties of the results the data suggest that not only the gamma photons but fast neutrons, too, induce thermoluminescence response of the 30 mol% Y_2O_3 ·vitroceramic. Furthermore, the obtained relative neutron sensitivities suggest a neutron energy dependent TL response of vitroceramic in the case of the $D_n = 1.5 - 85$ absorbed dose region.

Estimation of the TL dose response of the $30Y_2O_3 \cdot 30P_2O_5 \cdot 40SiO_2$ vitroceramic in mixed n - γ fields

Samples of the $30Y_2O_3 \cdot 30P_2O_5 \cdot 40SiO_2$ vitroceramics material were irradiated at the broad spectrum $d+Be$ and the quasi-monoenergetic $d+D$ neutron sources in mixed n - γ fields. The separate neutron and gamma absorbed dose were measured by the twin ionization chamber technique.

The task was the estimation of the separated TL_G and TL_N signals from the measured \overline{TL}_{N+G} signal, from the separate D_N and D_G absorbed dose and the beta/gamma TL sensitivity of the vitroceramic.

The estimated TL dose response of vitroceramic material in the mixed n - γ field of the $d+Be$ neutron source

The total absorbed doses were 2.75, 9.46 and 98.10 Gy. The gamma absorbed doses were 0.24, 1.34 and 13.91 Gy. The neutron absorbed doses were 2.51, 8.12 and 84.19 Gy. The result suggest that the dose response of the $30Y_2O_3 \cdot 30P_2O_5 \cdot 40SiO_2$ vitroceramics as a function of the total, neutron and gamma absorbed doses were linear within that uncertainties of the dosimetry measurements. **Figure 3-2** show the estimated dose response of the vitroceramics material as the function of the absorbed doses. The indicated uncertainties were obtained from the dosimetry measurements and the TL signals measurements.

The estimated dose response functions of vitroceramic material in the mixed n - γ field of the $d+D$ neutron source

The total absorbed doses were 1.67, 5.13 and 30.82 Gy. The gamma absorbed doses were 0.18, 0.63 and 5.27 Gy. The neutron absorbed doses were 1.49, 4.50 and 25.55 Gy. The result suggest that the dose response of the $30Y_2O_3 \cdot 30P_2O_5 \cdot 40SiO_2$ vitroceramics as function of the total, neutron and gamma absorbed doses were linear within that uncertainties of the dosimetry measurements. **Figure 3-2** show the estimated dose response of the vitroceramics material as

function of the absorbed doses. The plotted uncertainties were obtained from dosimetry measurements and the TL signals measurements.

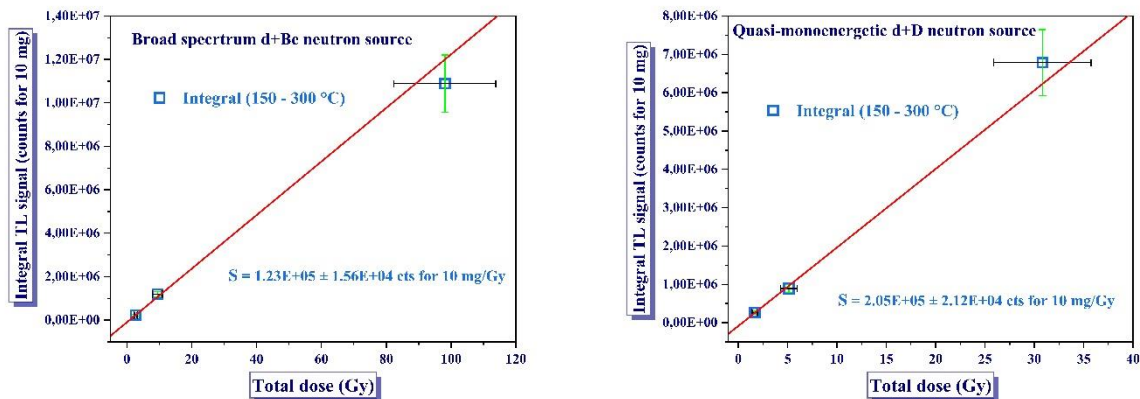


Figure 3-2. The TL dose response of the $30\text{Y}_2\text{O}_3\cdot 30\text{P}_2\text{O}_5\cdot 40\text{SiO}_2$ vitroceraamics material as function of the total absorbed dose (D_{N+G}).

4. Investigation of the TL of the neutron irradiated $30\text{Y}_2\text{O}_3\cdot 30\text{P}_2\text{O}_5\cdot 40\text{SiO}_2$ vitroceraamic with β^- -particles

The aims of the investigations were

- check if 80 -110 Gy neutron absorbed dose resulted in observable permanent alteration of the TL glow curve and dose response of the material or not,
- measurement of the TL response as a function of the β^- absorbed dose in the $D_\beta = 0.75 - 1000$ Gy absorbed dose range.

Samples 2&4 and Sample 3 were used for the studies. Samples 2&4 were never irradiated before and, hereinafter, they are referred to as the reference samples. Sample 3 had been irradiated with fast neutrons ($D_N \approx 100$ Gy) in earlier experiments.

Samples 2&4 and Sample 3 were exposed to low (0.75, 1.5, 3, 6, 9 and 15 Gy) and high (30, 45, 60, 80, 100, 200, 400, 500 and 1000 Gy) β^- absorbed doses at the $^{90}\text{Sr}\text{-}^{90}\text{Y}$ beta source (Risø TL/OSL Model TL/OSL-DA-20). Three irradiation experiments were carried out. It has to be emphasized that Sample 3 was not irradiated with 1000 Gy.

The TL glow curves of the vitroceraamic material and the TL response as the function of the β^- absorbed doses

The thermal treatment consisted of a preheat with a duration of 10 s at 175 °C. The integrated TL signals and TL glow curves were normalized to a mass of 10 mg for each aliquots.

The glow curves

The TL glow curve of the $30\text{Y}_2\text{O}_3 \cdot 30\text{P}_2\text{O}_5 \cdot 40\text{SiO}_2$ vitroc ceramic material had one peak with a maximum at around 220°C . The region of interest (ROI) of the TL glow curve had to be broadened when the absorbed dose was increased. In the cases of the 0.75, 1.5, 3, 6, 9 and 15 Gy absorbed doses the ROI selected for integration of the TL signals was the $150^\circ\text{C} - 300^\circ\text{C}$ temperature range. In the case of the 30 Gy absorbed dose the selected ROI was the 150°C to 350°C range. In the cases of 45, 60, 80 and 100 Gy absorbed doses the selected ROI was the $100 - 400^\circ\text{C}$ range. In the case of the 200 Gy absorbed dose the ROI selected for integration of the TL signals was the $100^\circ\text{C} - 450^\circ\text{C}$ temperature range. In the cases of 400, 500 and 1000

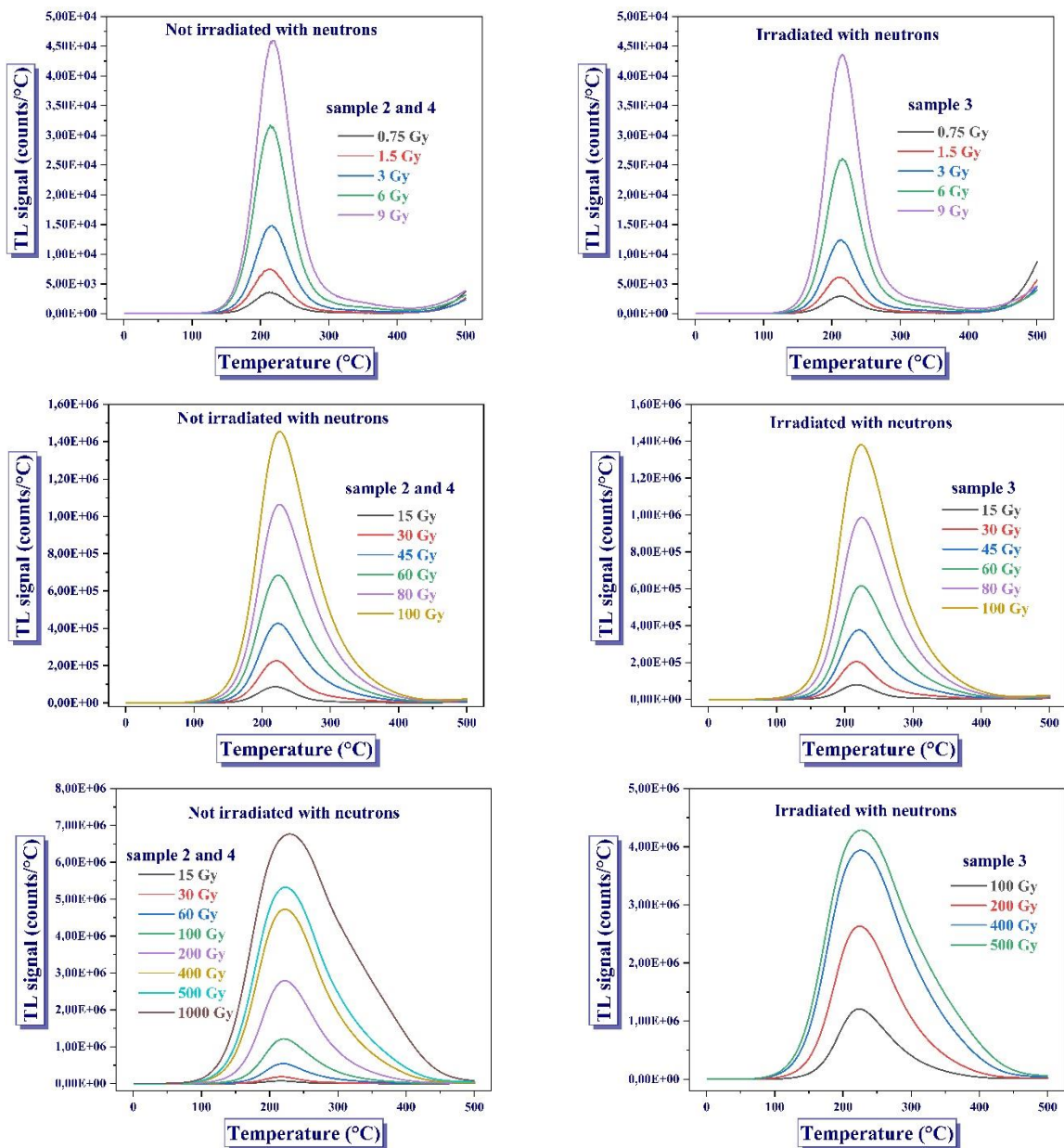


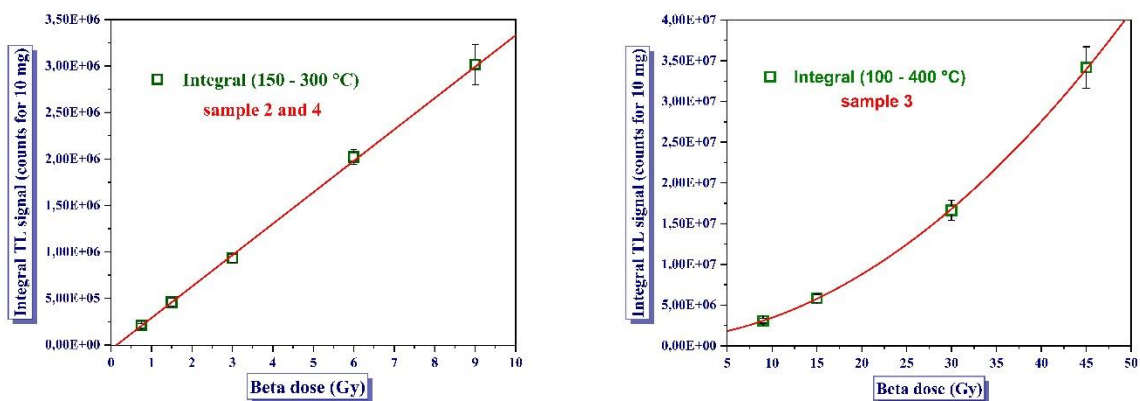
Figure 4-1. The averaged TL glow curves as a function of absorbed dose.

Gy absorbed dose the selected ROI was the 50 °C - 500 °C range. Each aliquot of the 30Y₂O₃·30P₂O₅·40SiO₂ vitroc ceramic material showed similar results as a function of absorbed dose. The relevant averaged TL glow curves of the aliquots are shown in **Figure 4-1**.

The dose response

On the basis of the results the 150 °C - 300 °C, 100 °C - 400 °C and 50 °C - 500 °C ranges were used for integration for obtaining the dose response of the TL signal, that is depend from the absorbed dose range.

In the absorbed dose range between 0.75 Gy and 9 Gy the dose responses of the Samples (Sample 2&4 and Sample 3) were linear. The sensibility of Sample 2&4 was $3.38 \text{ E}+05 \pm 6.77\text{E}+03$ cts for 10 mg/Gy. The sensibility of Sample 3 was $2.84\text{E}+05 \pm 8.60\text{E}+03$ cts for 10 mg/Gy. In the 9 Gy - 45 Gy range the dose responses of the Samples (Sample 2&4 and Sample 3) were not linear and a second order polynomial was fit to the data. In the 45 Gy - 100 Gy range the dose responses of the Samples (Sample 2&4 and Sample 3) were linear. The sensibility of the reference sample was $1.92 \text{ E}+06 \pm 7.28\text{E}+04$ cts for 10 mg/ Gy. The sensibility of the Sample 3 was $2.04 \text{ E}+06 \pm 1.17\text{E}+05$ cts for 10 mg/Gy. In the 15 Gy - 100 Gy range the dose responses of the Samples (Sample 2&4 and Sample 3) were not linear and a fourth degree polynomial was fit to the data. In the 0.75 Gy - 100 Gy range the dose responses of the Samples (Sample 2&4 and Sample 3) were not linear. No fit was found for the whole absorbed dose range. In the 100 Gy - 1000 Gy range the dose response of the Sample 2&4 was not linear and a second order polynomial was fit to the data. In the 100 Gy - 500 Gy range the dose response of the Sample 3 was not linear and a second order polynomial was fit to the data. **Figure 4-2** shows the representative dose response of Samples (Sample 2&4 and Sample 3) as a function of the β^- absorbed dose.



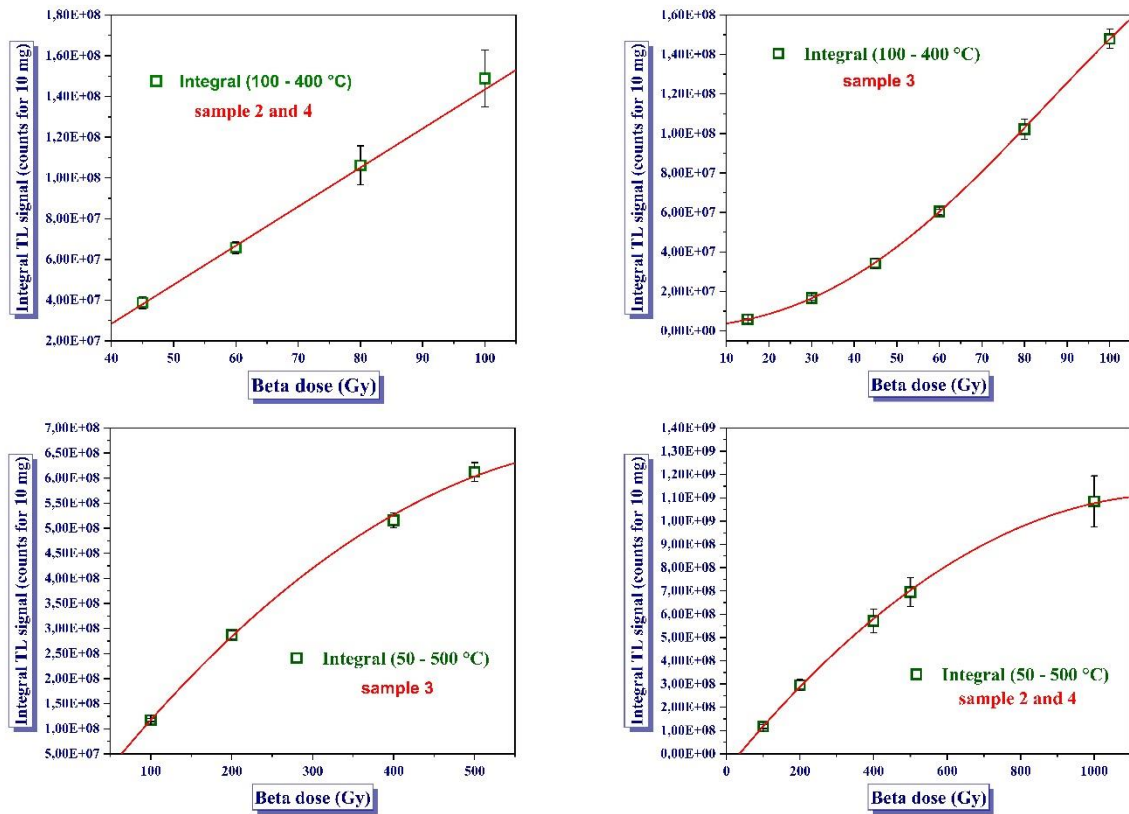


Figure 4-2. The representative dose response of Samples (Sample 2&4 and Sample 3).

Comparison the TL responses of the samples irradiated and not irradiated with fast neutrons

In the case of irradiations Sample 2&4 and Sample 3 were used and the obtained dose response functions were similar in the 0.75 - 1000 Gy range. **Figure 4-3** shows the comparison of the averaged dose response functions. The averaged TL signals are presented for the 0.75 Gy - 9 Gy range (a), for the 45 Gy - 100 Gy range (b), for the 15 Gy - 100 Gy range (c) and for the 100 Gy - 1000 Gy range (d).

In the 0.75 - 1000 Gy range the dose response functions of Sample 3 and Sample 2&4 are similar. The dose response of Sample 2&4 is non-linear in the 0.75 Gy - 1000 Gy range. The dose response of Sample 3 is non-linear in the 0.75 Gy - 500 Gy range and similar to the dose response of Samples 2&4 in this dose range. **Figure 4-4** shows the comparison of the averaged dose response functions. The averaged TL signals are presented for the 0.75 Gy - 1000 Gy range (a) and for the 0.75 Gy - 500 Gy range (b).

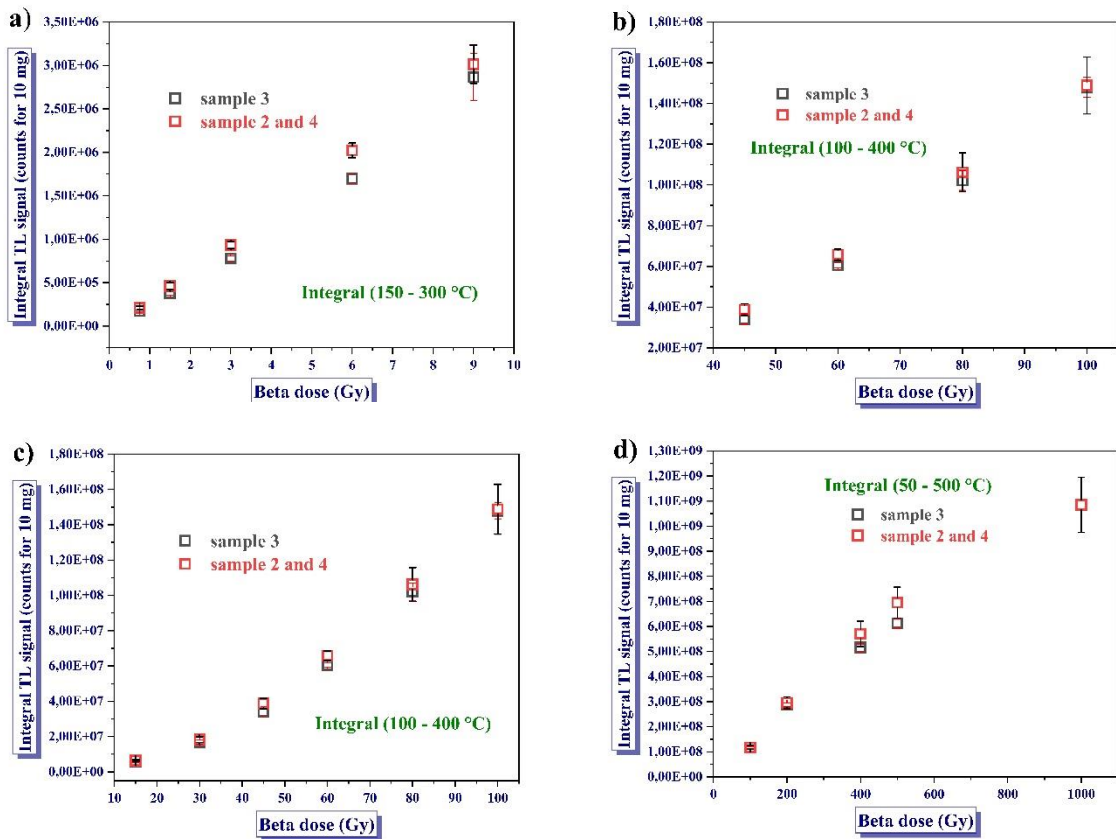


Figure 4-3. Comparison of the averaged dose response of Samples 2&4 and Sample 3.

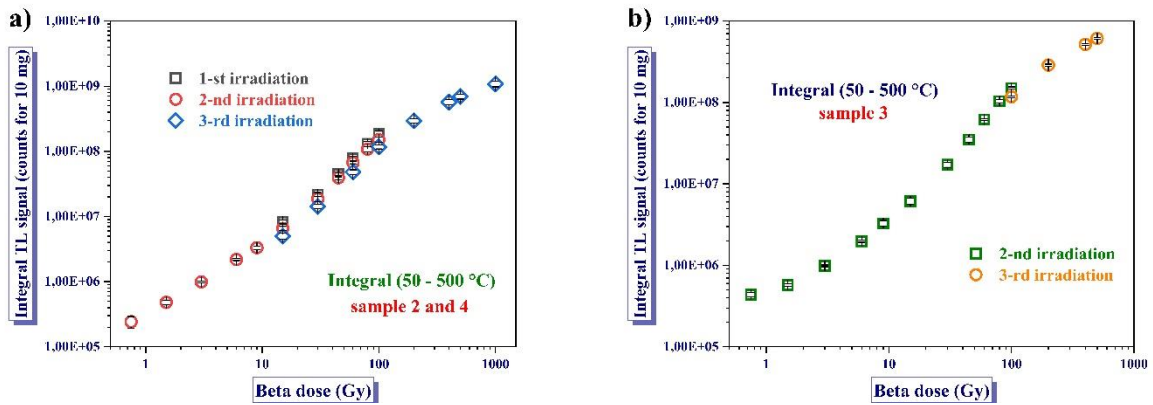


Figure 4-4. The dose response curve of Samples 2&4 and the Sample 3.

After reading out the aliquots of the samples each of them were irradiated individually again with the same β^- absorbed dose - chosen arbitrarily from the set of dose values used during the experiment. Then the TL signals were measured. In the case of each aliquot the TL signals obtained from dose response study were compared to the TL signals obtained from “repeat” (TL from study/TL from repeat). Furthermore, the ratio of the averaged TL signals of the

aliquots was calculated. The results obtained from the “repeat procedure” are shown in **Figure 4-5**. The TL signals ratio of each aliquots suggest statistical fluctuation and not a trend.

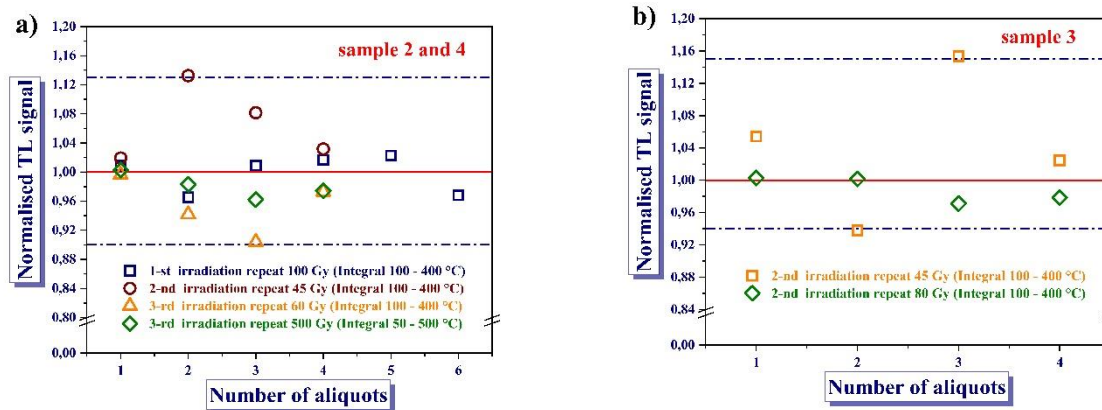


Figure 4-5. The results obtained from the “repeat procedure”.

We wanted to get information on the possible effect of the fast neutron induced displacement damage on the TL response of the 30 mol% Y_2O_3 vitroc ceramic to β^- particles. Therefore, the TL signals obtained from the dose response study done with Samples 2 and 4 (not irradiated with neutrons) and Sample 3 (irradiated with fast neutrons) were compared by calculating the $\xi = TL_{Samples\ 2\&4}/TL_{Samples\ 3}$ ratios. The TL signals of the samples were averaged and normalized to 10 mg mass. The β^- absorbed doses were $D_\beta = 0.75, 1.5, 3, 6, 9, 15, 30, 45, 60, 80, 100, 200, 400$ and 500 Gy. On the basis of the obtained results it can be concluded that the former irradiations with fast neutrons had no statistically significant effect on the TL response of the vitroc ceramics. The ratios from the three irradiations are presented in **Table 4-1**.

Table 4-1. The $\xi = TL_{Samples\ 2\&4}/TL_{Samples\ 3}$ ratios of the average TL signals as a function of the β^- absorbed dose.

Irradiation 1 at the ^{90}Sr - ^{90}Y source								
Dose (Gy)	60	100	100	Integration region				
ξ	0.914	0.909	0.911	100-400 °C				
Irradiation 2 at the ^{90}Sr - ^{90}Y source								
Dose (Gy)	0.75	1.5	3	6	9	15	Integration region	
ξ	1.213	1.180	1.179	1.184	1.047	1.093	150-300 °C	
Dose (Gy)	30	45	60	80	100	Integration region		
ξ	1.098	1.132	1.087	1.039	1.005	100-400 °C		
Irradiation 3 at the ^{90}Sr - ^{90}Y source								
Dose (Gy)	60*	60*	100*	200	400	500	500	Integration region
ξ	0.906	0.949	0.997	1.027	1.105	1.135	1.157	50-500 °C

*The TL signals were integrated between 100 and 400 °C.

5. Overview of the absorbed doses delivered to the 30 mol% Y₂O₃ vitroc ceramic

Table 5-1 summarized the beta absorbed doses delivered to the samples (1, 2, 3 and 4) by the ⁹⁰Sr-⁹⁰Y beta source.

Table 5-2 summarized the neutron and the gamma absorbed doses delivered to the samples (1, 2, 3 and 4) by the d+Be and d+D neutron sources.

Table 5-1. Beta absorbed doses delivered to the samples.

Radiation type	Number of irradiation	Sample 1	Sample 2	Sample 3	Sample 4
		Dose (Gy)	Dose (Gy)	Dose (Gy)	Dose (Gy)
β^- particles of ⁹⁰ Sr- ⁹⁰ Y	1	100	430	60	430
	2	40	395	475	410
	3	0	2865	1260	2865
Total β^- absorbed dose		140	3690	1795	3705

Table 5-2. The neutron and gamma absorbed doses delivered the samples (1, 2, 3 and 4) in the cases of the d+Be and the d+D neutron sources.

Radiation type	Number of irradiation	Sample 1		Sample 2		Sample 3		Sample 4	
		Dose (Gy)		Dose (Gy)		Dose (Gy)		Dose (Gy)	
		n	γ	n	γ	n	γ	n	γ
Mixed n- γ field of d+Be	1	2.51	0.24	0	0	2.51	0.24	0	0
	3	8.12	1.34	0	0	8.12	1.34	0	0
	5	84.19	13.91	0	0	84.19	13.91	0	0
Total n-γ absorbed dose		94.82	15.49	0	0	94.82	15.49	0	0
Mixed n- γ field of d+D	2	1.49	0.18	0	0	1.49	0.18	0	0
	4	4.50	0.63	0	0	4.50	0.63	0	0
	6	25.55	5.27	0	0	25.55	5.27	0	0
Total n-γ absorbed dose		31.54	6.08	0	0	31.54	6.08	0	0

II. CONCLUSIONS

Detailed comparative investigations of the nuclear radiation induced thermoluminescence properties of new types of xY₂O₃·(60-x)P₂O₅·40SiO₂ vitroc ceramics compounds doped with Y₂O₃ at various concentrations (x = 0, 5, 10, 15, 20, 30 mol%) was carried out. The 30Y₂O₃·30P₂O₅·40SiO₂ vitroc ceramic material gives the highest thermoluminescent response to unit absorbed dose of β^- particles, the following main conclusions can be drawn:

- the vitroc ceramics exhibited the less complicated glow curve structure;
- the dominant high-temperature peak presents the brightest signals and the best degree of linearity (from 0.75 Gy to 9 Gy);

- the material has acceptable batch homogeneity, poor fading of the signal, good repeatability and the minimum detectable absorbed dose is 4 mGy;
- it is a suitable candidate for dosimetry purposes.

From the study of the thermoluminescence properties of $30\text{Y}_2\text{O}_3\cdot 30\text{P}_2\text{O}_5\cdot 40\text{SiO}_2$ vitroceraamics in mixed n- γ fields, the following main conclusions can be drawn:

- the fast neutrons contributed to the thermoluminescency response of the 30 mol% Y_2O_3 ·vitroceraamics;
- the obtained results suggest neutron energy dependent relative neutron sensitivity of the material in the $D_n = 1.5 - 85$ absorbed dose region;
- in the case of d+Be neutrons ($E_n = 0 - 14.5$ MeV; $\bar{E}_n = 3.5$ MeV) the averaged relative neutron sensitivity of the vitroceraamics was $(\bar{k}_V)_{d+Be} = 0.032 \pm 7\%$;
- in the case of the d+D neutrons ($E_n = 12.4 \pm 0.22$ MeV) the obtained averaged relative neutron sensitivity of the vitroceraamics was $(\bar{k}_V)_{d+D} = 0.136 \pm 10\%$;
- in the cases of the d+Be and d+D neutron sources, the obtained results suggest that the estimated TL dose responses of the 30 mol% Y_2O_3 ·vitroceraamics as a function of the neutron, gamma and total absorbed doses are linear within the uncertainties of the dosimetry measurements;

I studied the possible effect of the fast neutron induced displacement damage on the TL response of the 30 mol% Y_2O_3 vitroceraamic to β^- particles, the following main conclusions can be drawn:

- the TL glow curves and the dose response of the non-irradiated and neutron irradiated samples of the 30 mol% Y_2O_3 vitroceraamics agreed within the uncertainty of the measurements;
- furthermore, the TL signal ratios of the non-irradiated and neutron irradiated samples of the 30 mol% Y_2O_3 vitroceraamics were fluctuated around 1;
- on the basis of the obtained results it can be concluded that no statistically significant effect of the neutron induced displacement damage on the TL properties of the material was observed.

Based on the obtained results it can be concluded that powder samples of the $30\text{Y}_2\text{O}_3\cdot 30\text{P}_2\text{O}_5\cdot 40\text{SiO}_2$ vitroceraamics are candidate for dosimetry purposes in radiation fields of β^- -particles, gamma photons and in mixed n- γ fields, too. Furthermore, the

$30\text{Y}_2\text{O}_3 \cdot 30\text{P}_2\text{O}_5 \cdot 40\text{SiO}_2$ thermoluminescent vitroceraamics is a good choice for monitoring the radiation damage of microelectronic devices (e.g. in MOSFETs) and fibre-optics systems that contain phosphosilicate glasses.

References

- [1] Glenn F. Knoll: Radiation detection and measurement, third edition, John Wiley & Sons, New York, United States of America, 2000.
- [2] J. Izewska and G. Rajan: Radiation dosimeters, Chapter 3 in International Atomic Energy Agency (IAEA), Technical Editor: E. B. Podgorsak: Radiation Oncology Physics: A Handbook for Teachers and Students, Printed by the IAEA, Vienna, Austria, p. 84-88, 2005.
- [3] Frank Herbert Attix: Introduction to radiological physics and radiation dosimetry, WILEY-VCH Verlag GmbH & Co. KGaA, 1986.
- [4] V. Kortov: Materials for thermoluminescent dosimetry: current status and future trends, Radiation Measurements, 42, 576–581, 2007.
- [5] S.W.S. McKeever: Thermoluminescence of Solids, Cambridge University Press, Cambridge, 1985.
- [6] S.W.S. McKeever, M. Moscovitch and P.D. Townsend: Thermoluminescence Dosimetry Materials: Properties and Uses, Nuclear Technology Publishing, Ashford 1995.
- [7] C. Furetta and P.-S. Weng: Operational Thermoluminescence Dosimetry, World Scientific Publishing Co. Pte. Ltd., Singapore, 1998.
- [8] C. Furetta, M. Prokić, R. Salomon and G. Kitis: Dosimetric characteristics of tissue equivalent thermoluminescent solid TL detectors based on lithium borate, Nuclear Instruments and Methods in Physics Research, 456, 411-417, 2001.
- [9] M. Prokić: Lithium Borate Solid TL Detectors, Radiation Measurements, 33, 393-396, 2001.
- [10] M. Santiago, C. Grasselli, E. Caselli, M. Lester, A. Lavat, and F. Spano: Thermoluminescence of SrB_4O_7 : Dy, Physica Status Solidi, 185, 285-289, 2001.
- [11] G.V. Rao, P.Y. Reddy and N. Veeraiyah: Thermoluminescence studies on $\text{Li}_2\text{O}-\text{CaF}_2-\text{B}_2\text{O}_3$ glasses doped with manganese ions, Materials Letter, 57, 403-408, 2002.

- [12] J. Li, J.Q. Hao, C.Y. Li, C.X. Zhang, Q. Tang, Y.L. Zhang, Q. Su and S.B. Wang: Thermally stimulated luminescence studies for dysprosium doped strontium tetraborate, *Radiation Measurements*, 39, 229-233, 2005.
- [13] S.S. Rojas, K. Yukimitu, A.S.S. de Camargo, L.A.O. Nunes and A.C. Hernandez: Undoped and calcium doped borate glass system for thermoluminescent dosimeter, *Journal of Non-Crystalline Solids*, 352, 3608-3612, 2006.
- [14] S.Y. Marzouk, F.H. Elbatal, A.M. Salem and S.M. Abo-Naf: Absorption spectra of gamma-irradiation TM-doped cabal glasses, *Optical Materials*, 29, 1456-1466, 2007.
- [15] E.M. Yoshimura, C.N. Santos, A. Ibanez and A.C. Hernandez: Thermoluminescent and optical absorption properties of neodymium doped yttrium aluminoborate and yttrium calcium borate glasses, *Optical Materials*, 31, 795-799, 2009.
- [16] M.M. Elkholy: Thermoluminescence of B_2O_3 - Li_2O glass system doped with MgO , *Journal of Luminescence*, 130, 1880-1892, 2010.
- [17] E. Tekin, A. Ege, T. Karali, P.D. Townsend and M. Prokic: Thermoluminescence studies of thermally treated $CaB_4O_7:Dy$, *Radiation Measurements*, 45, 764-767, 2010.
- [18] Y.S.M. Alajerami, S. Hashim, S.K. Ghoshal, M.A. Saleh, T. Kadni, M.I. Saripan, K. Alzimami, Z. Ibrahim and D.A. Bradley: The effect of TiO_2 and MgO on the thermoluminescence properties of a lithium potassium borate glass system, *Journal of Physics and Chemistry of Solids*, 74, 1816-1822, 2013.
- [19] H. Aboud, H. Wagiran, R. Hussin, H. Ali, Y. Alajerami and M.A. Saeed: Thermoluminescence properties of the Cu-doped lithium potassium borate glass, *Applied Radiation and Isotopes*, 90, 35-39, 2014.
- [20] M.M. Elkholy: Thermoluminescence for rare-earths doped tellurite glasses, *Materials Chemistry and Physics*, 77, 321-330, 2002.
- [21] J.S. Kim, A.K. Kwon, Y.H. Park, J.C. Choi, H.L. Park and G.C. Kim: Luminescent and thermal properties of full-color emitting $X_3MgSi_2O_8:Eu^{2+}, Mn^{2+}$ ($X=Ba, Sr, Ca$) phosphors for white LED, *Journal of Luminescence*, 122-123, 583-586, 2007.
- [22] M. Prokić and E.G. Yukihara: Dosimetric characteristics of high sensitive $Mg_2SiO_4:Tb$ solid TL detector, *Radiation Measurements*, 43, 463-466, 2008.
- [23] V. Pagonis, S. Mian, R. Mellinger and K. Chapman: Thermoluminescence kinetic study of binary lead-silicate glasses, *Journal of Luminescence*, 129, 570-577, 2009.

- [24] A. Timar-Gabor, C. Ivascu, S. Vasiliniuc, L. Daraban, I. Ardelean, C. Cosma and O. Cozar: Thermoluminescence and optically stimulated luminescence properties of the $0.5\text{P}_2\text{O}_5\text{-xBaO-(0.5-x)Li}_2\text{O}$ glass systems, *Applied Radiation and Isotopes*, 69, 780-784, 2011.
- [25] R.A. Barve, N. Suriyamurthy, B.S. Panigrahi and B. Venkatraman: Dosimetric investigations of Tb^{3+} -doped strontium silicate phosphor, *Radiation Protection Dosimetry*, doi: 10.1093/rpd/ncu226, 2014.
- [26] M.R. Chialanza, R. Keuchkerian, A. Cárdenas, A. Olivera, S. Vazquez, R. Faccio, J. Castiglioni, J.F. Schneider and L. Fornaro: Correlation between structure, crystallization and thermally stimulated luminescence response of some borate glass and glass-ceramics, *Journal of Non-Crystalline Solids*, 427, 191–198, 2015.
- [27] J. Park and R.S. Lakes: *Biomaterials - An introduction*, Springer, New York, 3rd edition, ISBN: B00177XGHY, 2007.
- [28] J.B. Park: *Biomaterials Science and Engineering*, Plenum Press, New York, ISBN: 978-1-4612-9710-9, 1984.
- [29] Claudio Furetta: *Handbook of Thermoluminescence*, World Scientific Publishing Co. Pte. Ltd., Singapore, 2003.
- [30] **B. Biró**, A. Pascu, A. Timar-Gabor and V. Simon: Thermoluminescence investigations on $x\text{Y}_2\text{O}_3\cdot(60-x)\text{P}_2\text{O}_5\cdot 40\text{SiO}_2$ vitroceramics, *Applied Radiation and Isotopes*, 98, 49-53, 2015.
- [31] Douglas D. DiJulio, Nataliia Cherkashyna, Julius Scherzinger, Anton Khaplanov, Dorothea Pfeiffer, Carsten P. Cooper-Jensen, Kevin G. Fissum, Kalliopi Kanaki, Oliver Kirstein, Georg Ehlers, Franz X. Gallmeier, Donald E. Hornbach, Erik B. Iverson, Robert J. Newby, Richard J. Hall-Wilton and Phillip M. Bentley: Characterization of the radiation background at the Spallation Neutron Source, VI European Conference on Neutron Scattering (ECNS2015), *Journal of Physics: Conference Series*, 746, 012033, 2016.
- [32] Homepage of International Fusion Materials Irradiation Facility (IFMIF). <http://www.ifmif.org/>
- [33] Yuefeng Qiu, Frederik Arbeiter, Ulrich Fischer and Florian Schwab: IFMIF-DONES HFTM neutronics modelling and nuclear response analyses, *Nuclear materials and Energy*, 15, 185-189, 2018.

- [34] International Thermonuclear Experimental Reactor (ITER) homepage, ITER Organization, 2018. <https://www.iter.org/proj/inafewlines>
- [35] **B. Biró**, A. Fenyvesi, A. Timar-Gabor and V. Simon: Thermoluminescence properties of $30\text{Y}_2\text{O}_3\cdot 30\text{P}_2\text{O}_5\cdot 40\text{SiO}_2$ vitroceraamics in mixed neutron-gamma fields, *Applied Radiation and Isotopes*, 135, 224–231, 2018.
- [36] J.K. Christie, J. Malik and A. Tilocca: Bioactive glasses as potential radioisotope vectors for in situ cancer therapy: investigating the structural effects of yttrium, *Physical Chemistry Chemical Physics*, 13, 17749–17755, 2011.
- [37] Y. Fu and J. K. Christie: Atomic structure and dissolution properties of yttrium containing phosphate glasses, *International Journal of Glass Science*, available online at DOI: 10.1111/ijag.12325, 2017.
- [38] H.J. Brede, G. Dietze, K. Kudo, U.J. Schrewe, F. Tancu and C. Wen: Neutron yields from thick be targets bombarded with deuterons or protons, *Nuclear Instruments and Methods in Physics Research A*, 274, 332-344, 1989
- [39] Peter Reimer: Fast neutron induced reactions leading to activation products: selected cases relevant to development of low activation materials, transmutation and hazard assessment of nuclear wastes, Doctoral degrees, The Faculty of Mathematics and Natural Sciences, The University of Cologne, Print shop of research center Jülich, 2002.
- [40] S.Y.F. Chu, L.P. Ekström and R.B. Firestone: The Lund/LBNL Nuclear Data Search, Version 2.0, 1999. (<http://nucleardata.nuclear.lu.se/toi/>)
- [41] M.B. Chadwick, M. Herman, P. Obložinský, M.E. Dunn, Y. Danon, A.C. Kahler, D.L. Smith, B. Pritychenko, G. Arbanas, R. Arcilla, R. Brewer, D.A. Brown, R. Capote, A.D. Carlson, Y.S. Cho, H. Derrien, K.Guber, G.M. Hale, S. Hoblit, S. Holloway, T.D. Johnson, T. Kawano, B.C. Kiedrowski, H. Kim, S. Kunieda, N.M. Larson, L. Leal, J.P. Lestone, R.C. Little, E.A. McCutchan, R.E. MacFarlane, M. MacInnes, C.M. Mattoon, R.D. McKnight, S.F. Mughabghab, G.P.A. Nobre, G. Palmiotti, A. Palumbo, M.T. Pigni, V.G. Pronyaev, R.O. Sayer, A.A. Sonzogni, N.C. Summers, P. Talou, I.J. Thompson, A. Trkov, R.L. Vogt, S.C. van der Marck, A. Wallner, M.C. White, D. Wiarda, and P.G. Young: ENDF/B-VII.1 Nuclear Data for Science and Technology: Cross Sections, Covariances, Fission Product Yields and Decay Data. *Nuclear Data Sheets* 112, 2887-3152, 2011. (<http://www.nndc.bnl.gov/sigma/index.jsp>)

- [42] G. Székely: FGM - A flexible gamma-spectrum analysis program for a small computer, *Computer Physics Communications*, 34, 313-324, 1985.
- [43] J. J. Broerse, B. J. Mijnheer and J. R. Williams, European Clinical Neutron Dosimetry Group (ECNEU): European protocol for neutron dosimetry for external beam therapy, *British Journal of Radiology*, 54, 882-898, 1981.
- [44] P. Wootton, P. Almond, F.H. Attix, M. Awschalom, P. Bloch, J. Eenmaa, L. Goodman, R. Graves, J. Horton, F. Kuchnir, J. McDonald, V. Otte, P. Shapiro, J. Smathers, N. Suntharalingam and F. Waterman, Fast Neutron Beam Dosimetry Physics Radiation Therapy Committee: PROTOCOL FOR NEUTRON BEAM DOSIMETRY, AAPM REPORT No. 7, Task Group No. 18, American Association of Physicists in Medicine by the American Institute of Physics, New York, United States of America, 1-45, 1980.
- [45] R. F. Shonka, J. E. Rose, and G. Failla: "Conducting plastic equivalent to tissue, air and polystyrene," in *Second United Nations International Conference on Peaceful Uses of Atomic Energy*. New York: United Nations, 1958, p. 160.
- [46] M. B. Chadwick, H. H. Barschall, R. S. Caswell, P. M. DeLuca, G. M. Hale, D. T. L. Jones, R. E. MacFarlane, J. P. Meulders, H. Schuhmacher, U. J. Schrewe, A. Wambersie and P. G. Young: A consistent set of neutron kerma coefficients from thermal to 150 MeV for biologically important materials. *Medical Physics* 26, 974-991, 1999.